Real-Case Simulations of Hurricane–Ocean Interaction Using A High-Resolution Coupled Model: Effects on Hurricane Intensity

MORRIS A. BENDER

NOAA/Geophysical Fluid Dynamics Laboratory, Princeton University, Princeton, New Jersey

ISAAC GINIS

Graduate School of Oceanography, University of Rhode Island, Narragansett, Rhode Island

(Manuscript received 13 July 1998, in final form 2 April 1999)

ABSTRACT

In order to investigate the effect of tropical cyclone–ocean interaction on the intensity of observed hurricanes, the GFDL movable triply nested mesh hurricane model was coupled with a high-resolution version of the Princeton Ocean Model. The ocean model had $\frac{1}{6}^\circ$ uniform resolution, which matched the horizontal resolution of the hurricane model in its innermost grid. Experiments were run with and without inclusion of the coupling for two cases of Hurricane Opal (1995) and one case of Hurricane Gilbert (1988) in the Gulf of Mexico and two cases each of Hurricanes Felix (1995) and Fran (1996) in the western Atlantic. The results confirmed the conclusions suggested by the earlier idealized studies that the cooling of the sea surface induced by the tropical cyclone will have a significant impact on the intensity of observed storms, particularly for slow moving storms where the SST decrease is greater. In each of the seven forecasts, the ocean coupling led to substantial improvements in the prediction of storm intensity measured by the storm's minimum sea level pressure.

Without the effect of coupling the GFDL model incorrectly forecasted 25-hPa deepening of Gilbert as it moved across the Gulf of Mexico. With the coupling included, the model storm deepened only 10 hPa, which was much closer to the observed amount of 4 hPa. Similarly, during the period that Opal moved very slowly in the southern Gulf of Mexico, the coupled model produced a large SST decrease northwest of the Yucatan and slow deepening consistent with the observations. The uncoupled model using the initial NCEP SSTs predicted rapid deepening of 58 hPa during the same period.

Improved intensity prediction was achieved both for Hurricanes Felix and Fran in the western Atlantic. For the case of Hurricane Fran, the coarse resolution of the NCEP SST analysis could not resolve Hurricane Edouard's wake, which was produced when Edouard moved in nearly an identical path to Fran four days earlier. As a result, the operational GFDL forecast using the operational SSTs and without coupling incorrectly forecasted 40-hPa deepening while Fran remained at nearly constant intensity as it crossed the wake. When the coupled model was run with Edouard's cold wake generated by imposing hurricane wind forcing during the ocean initialization, the intensity prediction was significantly improved. The model also correctly predicted the rapid deepening that occurred as Fran began to move away from the cold wake. These results suggest the importance of an accurate initial SST analysis as well as the inclusion of the ocean coupling, for accurate hurricane intensity prediction with a dynamical model.

Recently, the GFDL hurricane–ocean coupled model used in these case studies was run on 163 forecasts during the 1995–98 seasons. Improved intensity forecasts were again achieved with the mean absolute error in the forecast of central pressure reduced by about 26% compared to the operational GFDL model. During the 1998 season, when the system was run in near–real time, the coupled model improved the intensity forecasts for all storms with central pressure higher than 940 hPa although the most significant improvement (~60%) occurred in the intensity range of 960–970 hPa. These much larger sample sets confirmed the conclusion from the case studies, that the hurricane–ocean interaction is an important physical mechanism in the intensity of observed tropical cyclones.

1. Introduction

There has been a steady improvement in tropical cyclone track forecasting over the last two decades, mostly due to improvements in dynamical models and satellite observations (Lawrence et al. 1997). In spite of the increase in the skill of hurricane motion forecasts, there appears to be little skill in predicting hurricane intensity changes. One of the potentially significant constraints on the dynamical prediction of tropical cyclone intensity is due to a lack of knowledge about the ocean response to the storm forcing and our understanding of the coupled ocean–atmosphere system. For the vast majority of

Corresponding author address: Dr. Morris Bender, NOAA/GFDL, Princeton University, Forrestal Campus, U.S. Route 1, Princeton, NJ 08542.
E-mail: mb@gfdl.gov

research and operational dynamical models, conditions of fixed sea surface temperature (SST) in time is assumed. Yet numerous observational and numerical studies have confirmed that an important positive and negative feedback mechanism exists in the tropical cyclone–ocean system. As the tropical cyclone intensifies, the evaporation rate increases due to the larger wind speeds, leading to an increase in the latent energy supply that drives the circulation of the tropical cyclone. This represents a positive feedback process. Strong turbulent mixing also develops in the upper ocean in response to the increasing wind stress. This causes a decrease in the SSTs due to entrainment of the cooler waters from the thermocline into the mixed layer representing a negative feedback mechanism.

The SST decrease induced by tropical cyclones have been observed to vary from 1° to about 6°C (Black 1983). Bender el al. (1993a, hereafter BGK), summarized the maximum sea surface cooling observed after the passage of 16 tropical cyclones. In that study, the observations were grouped according to slow, medium, and fast moving storms, with average cooling for the three groups of 5.3°, 3.5° and 1.8°C, respectively. This amount of SST decrease underneath the hurricane can significantly reduce the heat and moisture fluxes at the sea surface, which may play an important role in the storm evolution. Not surprisingly, air–sea interaction in tropical cyclones has become an important scientific and practical problem for investigation in recent years.

In early numerical studies of the tropical cyclone–ocean interaction using axisymmetric models (Chang and Anthes 1979; Sutyrin and Khain 1979) the SST cooling did not have a large effect on the tropical cyclone intensity. Using simple three-dimensional coupled models (e.g., Sutyrin and Khain 1984; Ginis et al. 1989) the initial response of the tropical cyclone to the SST decrease was delayed with significant impact on the storm intensity (i.e., weakening of 5–7 hPa) occurring on the second day of integration. However, all these previous integrations were performed with coarse resolution of 40–60 km. In BGK the tropical cyclone–ocean interaction was investigated more thoroughly using a high-resolution coupled model in which the Geophysical Fluid Dynamics Laboratory (GFDL) tropical cyclone research model was coupled with a multilayer primitive equation ocean model. In this study a set of idealized numerical experiments were performed in which a tropical cyclone vortex was embedded in both easterly and westerly basic flows or no initial basic flow. The experiments indicated that the cooling of the SST induced by the tropical cyclone resulted in a significant decrease in storm intensity due to the reduction of total heat flux into the tropical cyclone circulation. Consistent with the observational studies, the sea surface cooling was found to be larger when the storms moved slower, resulting in the largest decrease in storm intensity compared to experiments run without the effect of the coupling included. Similar results were obtained by Khain and Ginis (1991) and Falkovich et al. (1995). More recently, idealized simulations (Hodur 1997) were performed using coupled and noncoupled versions of the Naval Research Laboratory's nonhydrostatic Coupled Ocean–Atmosphere Mesoscale Prediction System. Although performed for idealized storms, these results suggested that the tropical cyclone–ocean interaction likely played an important role in intensity in real storms as well. However, analysis of numerical simulations involving observed cases was still necessary to clarify the role of the tropical cyclone–ocean interaction in the real atmosphere and ocean.

The primary goal of the present study is to examine the effects of the tropical cyclone–ocean interaction on the intensity of observed storms by coupling the GFDL hurricane model with a high-resolution version of the Princeton Ocean Model (Blumberg and Mellor 1987). It is hoped that this study will thus serve to verify the conclusions suggested by the earlier idealized studies regarding the effect of tropical cyclone–ocean interaction on observed storms.

In the early 1990s, the uncoupled version of the GFDL hurricane research model was incorporated into a new hurricane prediction system (Kurihara et al. 1995). Beginning in 1995 the GFDL hurricane prediction system became the new official operational hurricane prediction model for the National Weather Service and is currently run at the National Centers for Environmental Prediction (NCEP) for all tropical cyclones in both the east Pacific and Atlantic basins during the hurricane season. The forecast system has performed very well in providing accurate track forecasts (Kurihara et al. 1998). As far as intensity prediction is concerned, the performance of the model has shown little skill as it has exhibited a tendency to overintensify weak storms and underintensify strong systems (Fig. 1). The large intensity errors during the 12–24-h forecast period (Fig. 1, top) suggest that one of the problem areas with the model's intensity forecasts during the early forecast period is likely associated with the model initialization, especially with the axisymmetric assumption in the specification of the initial storm structure (Kurihara et al. 1998). Recently, an improvement in the initialization technique has begun to be evaluated, which combines the model forecasted asymmetries obtained from the previous forecast with the axisymmetric component computed from the current storm message file. Results have suggested that inclusion of the asymmetric component in the initial storm structure may lead to reduction in the intensity error for the 12- and 24-h forecasts particularly for storms below hurricane strength. Another possible source of error in the intensity prediction is the $\frac{1}{6}^\circ$ resolution of the innermost grid, which is still insufficient to adequately resolve the interior storm structure. As indicated by Fig. 1, with the current model resolution the model-predicted surface winds seldom exceeded 100 kt. On the other hand, the results of BGK also strongly suggest that the inclusion of the effect of

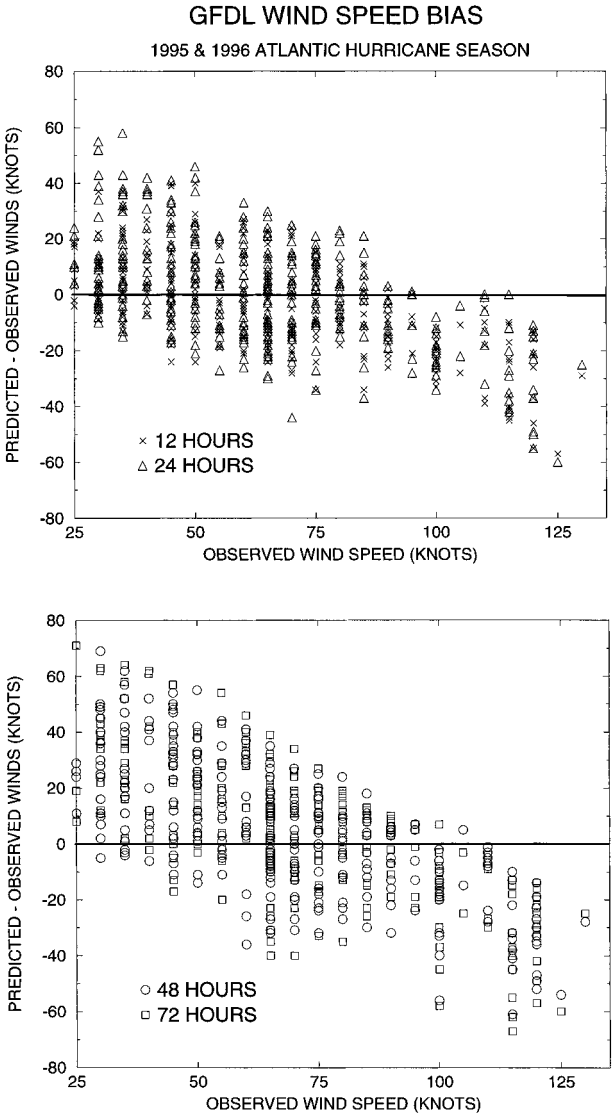

FIG. 1. Distribution of the wind error (predicted − observed wind speed) in kt, from the GFDL prediction system, for all Atlantic cases during the 1995 and 1996 seasons and plotted as a function of the observed wind speed. The 12- and 24-h forecast wind errors (top) and the 48- and 72-h forecast errors (bottom) are combined and plotted together.

ocean interaction is also of critical importance for intensity prediction and that intensity forecasts of storms may be significantly improved in many cases with this effect included in the GFDL prediction system. This will be addressed in detail throughout the present study. It is likely that all three of these problem areas as well as other limitations in the model physics will have to be adequately resolved before skillful intensity forecasts are routinely possible with the model.

The version of the GFDL hurricane model used for this study is identical to the one run operationally by the National Weather Service with the addition of the ocean coupling. A brief description of the tropical cyclone and ocean models will be presented in section 2. The steps used in the initialization of the ocean model will also be described in detail. Next, the numerical results will be shown in section 3 focusing first on Hurricanes Gilbert and Opal in the Gulf of Mexico and second on Hurricanes Felix and Fran in the Atlantic. Finally, a summary of the results and concluding remarks will be presented in section 4.

TABLE 1. Grid system of the triply nested mesh hurricane model.

Mesh	Grid resolution (°)	Domain size: Longitude (°)	Domain size: Longitude Points	Domain size: Latitude (°)	Domain size: Latitude Points	Time step (s)
1	1	75	(75)	75	(75)	90
2	1/3	11	(33)	11	(33)	30
3	1/6	5	(30)	5	(30)	15

2. Model description, initialization, and experimental design

a. Tropical cyclone model description

The multiply nested moveable mesh model described in detail by Kurihara et al. (1998) was used for all of the time integrations of the tropical cyclone model. The model is a primitive equation model formulated in latitude, longitude, and sigma (σ) coordinates, with 18 levels in the vertical (i.e., Table 1 of Kurihara et al. 1998). The grid system for each of the triply nested meshes in the present study is summarized in Table 1. The outermost domain is stationary during the integrations, and ranged from 10°S to 65°N in the meridional direction, and was positioned in the zonal direction depending on the storm's initial and 72-h official forecasted position determined by the National Hurricane Center. The two inner meshes are movable and follow the storm center.

The model physics include cumulus parameterization described by Kurihara (1973) with some additional modifications (Kurihara and Bender 1980, appendix C), a Monin–Obukhov scheme for the surface flux calculation, and the Mellor and Yamada (1974) level-two turbulence closure scheme for the vertical diffusion, with a background diffusion coefficient added. As described by Tuleya (1994), the Schwarzkopf and Fels (1991) infrared and Lacis and Hansen (1974) solar radiation parameterizations were also incorporated, with interactive radiative effects of clouds and a diurnal radiation cycle. The land surface temperature was computed by an energy equation containing a soil layer. The capability of this model has been clearly demonstrated both operationally and as a research model (e.g., Kurihara et al. 1998).

The initial condition for the hurricane model was determined from the hurricane model initialization scheme described in Kurihara et al. (1995), which uses the

NCEP T126 global analysis and the storm message provided by the National Hurricane Center. In the current GFDL initialization procedure the initial storm structure is estimated from the data in the storm message. This provides the target wind field for generation of the tropical cyclone vortex using an axisymmetric version of the prediction model. The symmetric vortex and an asymmetric component, which approximates the contribution due to the beta effect, is then merged back into the environmental fields determined from the global analysis. This is the identical initialization procedure that is currently used operationally (Kurihara et al. 1998). Forecast fields from the NCEP global model were then obtained to specify the time-dependent lateral boundary used during each of the forecasts.

b. Ocean model description

The importance of the oceanic feedback mechanism in the dynamics of tropical cyclones suggests the need for realistic modeling of the ocean response. The upper ocean is ageostrophic and highly diabatic with vertical and horizontal mixing processes occurring in both the well-stirred mixed layer near the surface and in the stratified region below. The vertical mixing mainly determines the degree of ocean response to a tropical cyclone (e.g., Price 1981; Ginis and Dikinov 1989). Therefore, for proper simulation of the ocean interaction, the ocean model must have highly accurate representation of upper ocean mixed layer physics. For this reason the model used for the coupled hurricane–ocean simulations presented in this study was the Princeton Ocean Model (POM) developed by Blumberg and Mellor (1987). This model is widely distributed to the academic community and industry and is run semioperationally as part of the Coastal Ocean Forecast System at NCEP. The latest version of the model is described in detail by Mellor (1998) and therefore only briefly outlined here.

The POM is a three-dimensional, primitive equation model with complete thermohaline dynamics. It has an ocean-bottom-following, sigma vertical coordinate system and a free surface. Thus it is capable of resolving the coastal areas adjacent to the deep ocean, including the continental shelf and slope. Most important for hurricane simulations, a second-order turbulence closure scheme (Mellor and Yamada 1982) is embedded in the model to provide mixing parameters so that surface mixed layer dynamics are well represented. The momentum, heat, and turbulent kinetic energy equations are solved and the prognostic variables of the free surface, potential temperature, salinity, and velocity, are calculated. The horizontal diffusion terms are calculated using the scales of motion resolved by the model and the local deformation field (Smagorinsky 1963). The density is calculated using the modified United Nations Educational, Scientific, and Cultural Organization (UNESCO) equation of state (Mellor 1991).

c. Experimental design

Two ocean model computational domains were set up for the present study. The first one spanned the region from 18° to 31°N and from 78° to 98°W, and included all of the Gulf of Mexico, the northwestern portion of the Caribbean Basin, and the southwestern portion of the South Atlantic Bight (e.g., Fig. 2). The second domain covered the area from 17° to 47°N and 50° to 82°W in the western Atlantic (e.g., Fig. 13).

Since accurate simulation of the interaction between a tropical cyclone and ocean requires the use of a very high resolution atmosphere–ocean model, horizontal resolution of $\frac{1}{6}^\circ$ was used for both ocean domains. This matched the finest resolution of the hurricane model and was sufficient to resolve the fine- to mesoscale structure of the hurricane-induced currents. Since the vertical turbulent mixing is a primary cause for the sea surface cooling, adequate representation of this process required a very high resolution in the vertical. The number of vertical layers was set at 21 for the Gulf of Mexico and 23 for the western Atlantic, with higher resolution in the upper mixed layer (Table 2), which enabled the upper ocean dynamics to be represented with greater accuracy.

The bottom topography was constructed from ETOPO5 5-min gridded ocean depth coverage by the National Geophysical Data Center and interpolated onto the model grid system. At the shore boundary the model's minimum depth is 10 m. A special treatment was required in the areas with very steep topography where potentially significant pressure gradient errors might be generated due to the use of sigma coordinates. To reduce the sigma coordinate truncation error a special smoother as suggested in Mellor et al. (1994) was applied to the bottom topography in each domain.

Both of the ocean computational domains had *closed* land–water boundaries and *open* lateral boundaries where the domains were surrounded by the sea. At the closed boundaries, a no-slip condition was invoked on the velocity field and there were no gridscale or subgridscale normal fluxes of any quantity. At the open boundaries, transport and thermal conditions were specified and prescribed according to observations where available (Leaman et al. 1987; Richardson 1985; Hogg et al. 1986) and using diagnostic calculations (Mellor et al. 1982). The transports specified at the open boundaries are summarized in Table 3, for both computational domains. The vertical distribution of normal velocities at the open boundaries were governed by the Sommerfeld radiation condition. The temperature and the salinity at inflow open boundaries were set according to the observed climatology.

Finally, for the coupled experiments, the method of coupling between the tropical cyclone and the ocean model was similar to the procedure used in BGK. During the period of one ocean model time step (i.e., 900 s), the tropical cyclone model, with 90-, 30-, and 15-s time

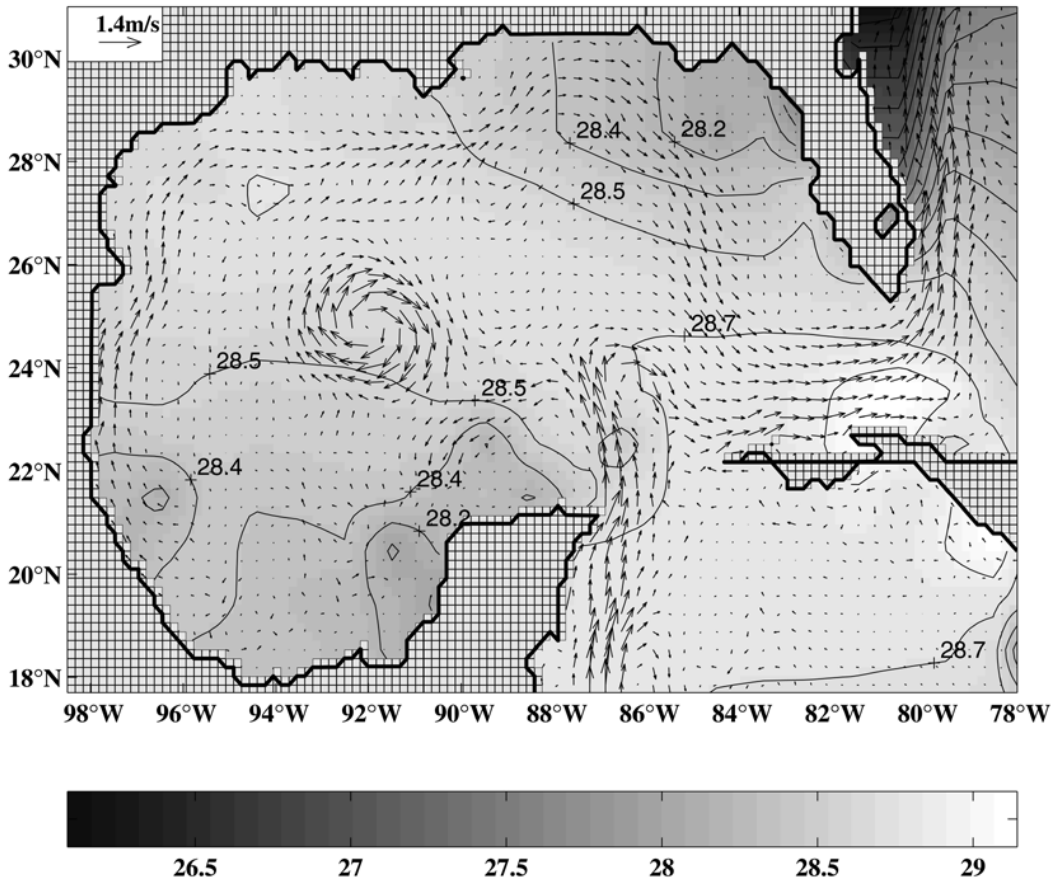

FIG. 2. SST (°C) and ocean surface currents in the Gulf of Mexico after the third step of the ocean initialization and assimilation of the warm-core eddy for the forecast of Hurricane Gilbert (1200 UTC 14 Sep 1988). The contour interval is 0.1°C with the lower SSTs indicated by the darker shading. The ocean model domain for the forecasts in the Gulf is shown.

steps (Table 1), was integrated keeping the SST constant. The wind stress, heat, moisture, and radiative fluxes computed in the tropical cyclone model were passed into the ocean model. The ocean model was then integrated one step and a new SST was calculated. The new SST was used in the ensuing time steps of the tropical cyclone model. In regions outside of the ocean domains, the SST field remained fixed in time. The transfer of the wind stress, heat, moisture, and radiative fluxes from the tropical cyclone model to the fixed grid system of the ocean model as well as the transfer of the SST field from the ocean to the tropical cyclone model were accomplished through bilinear interpolation.

d. Ocean model initialization

The importance of a realistic ocean and hurricane initialization for proper simulation of the ocean response and hurricane evolution in the coupled hurricane–ocean system cannot be overemphasized. The current operational GFDL hurricane model uses the real-time SST data derived from the operational global analysis produced by NCEP. These data consist of all SST observations available to NCEP (e.g., ship and buoy) within 10 h of observation time, combined with weekly averaged SST retrievals produced by the Advanced Very High Resolution Radiometer (AVHRR) carried aboard the National Oceanic and Atmospheric Administration (NOAA) Polar Orbiting Environmental Satellites. The ship, buoy, and satellite SST data are blended daily using optimum interpolation on a 1° lat–long spatial grid (Reynolds and Smith 1994). This resolution is too coarse, however, to capture large horizontal gradients in surface temperature on smaller spatial scales, especially over the continental shelf and slope. Presently, plans are being made to use higher-resolution data of 50 km produced operationally by NOAA's National Environmental Satellite, Data and Information Service (NESDIS). However, the interaction between the ocean and hurricane is largely controlled not only by the SST but also by other properties of the upper ocean such as the mixed layer depth and stratification in the upper thermocline and upper ocean currents. There is no real-time subsurface ocean data in advance of hurricanes that

TABLE 2. Summary of vertical sigma levels in the ocean model and depths (m) in the deepest regions of the Gulf of Mexico and western Atlantic.

	Gulf of Mexico		Western Atlantic	
K level	Sigma	Depth	Sigma	Depth
1	−0.0017	−5	−0.0009	−5
2	−0.0050	−15	−0.0027	−15
3	−0.0083	−25	−0.0045	−25
4	−0.0117	−35	−0.0064	−35
5	−0.0150	−45	−0.0082	−45
6	−0.0183	−55	−0.0100	−55
7	−0.0217	−65	−0.0118	−65
8	−0.0250	−75	−0.0141	−77.5
9	−0.0283	−85	−0.0168	−92.5
10	−0.0317	−95	−0.0200	−110
11	−0.0417	−125	−0.0245	−135
12	−0.0583	−175	−0.0318	−175
13	−0.0833	−250	−0.0455	−250
14	−0.1250	−375	−0.0682	−375
15	−0.1833	−550	−0.1000	−550
16	−0.2583	−775	−0.1409	−775
17	−0.3667	−1100	−0.2000	−1100
18	−0.5167	−1550	−0.2818	−1550
19	−0.7000	−2100	−0.3818	−2100
20	−0.9000	−2700	−0.5091	−2800
21	−1.0000	−3000	−0.6727	−3700
22			−0.8818	−4850
23			−1.0000	−5500

is operationally available at the present time. Therefore, the ocean initialization in this study must rely on a diagnostic and prognostic spinup of the ocean circulation using available climatological ocean data in combination with real-time SST data. For this study, the ocean model in the coupled system was initialized by utilizing the monthly averaged profiles of temperature and salinity produced by the NAVOCEANO Generalized Digital Environmental Model (GDEM). GDEM is an ocean climatology at 0.5° resolution created from the U.S. Navy observational database, which contains about five million observations worldwide dating back to 1920. The GDEM data provided the starting fields of temperature and salinity for the ocean model while the initial velocity field was set to zero.

The initialization procedure included four steps. First, the ocean model was integrated for one month in diagnostic mode (e.g., holding the temperature and salinity constant while allowing the velocity field to evolve in a natural and consistent manner) without surface forcing. This was followed by a three-month prognostic run in which the GDEM temperature and salinity at the sea surface were fixed in time and wind stress forcing from the Comprehensive Ocean–Atmosphere Data Set (COADS) was applied. These first two steps generated a monthly model climatology on the specified high-resolution grid system for those months for which the hurricane forecast experiments were made. The important facet of the ocean initialization is that it is forced by a set of fairly general, but quite realistic, inflow/outflow open ocean boundary conditions, which set up the influence of the large-scale ocean circulation (Table 3). This is especially important for initialization of ocean fronts such as the Loop Current in the Gulf of Mexico and the Gulf Stream in the western Atlantic.

The third and fourth steps of the initialization procedure involved adjusting the upper ocean structure to a more realistic prestorm condition at the start of the hurricane forecast. In the beginning of the third step, the sea surface temperature field from the NCEP operational global analysis was assimilated. The assimilation procedure involved replacement of the GDEM temperatures in the upper ocean mixed layer by the NCEP SSTs and prognostic model integration for another 10 days for dynamical adjustment. During this integration the NCEP temperature at the surface was kept constant and the COADS wind stress was applied.

During the final step, the cold wake at the sea surface produced by the hurricane three days prior to the start of the coupled model integration was generated. This step was necessary since the cold wake was not resolved with the 1° resolution NCEP SST analysis. It is anticipated that this may be partly remedied in the future as high-resolution SST analyses become available on a routine basis. In order to create the cold wake and the associated subsurface ocean temperature and current fields, the ocean model was forced by prescribed hurricane wind stress forcing, which was added to the

TABLE 3. Transports specified on the open boundaries of the western Atlantic and Gulf of Mexico domains in Sverdrups (1 Sv = 10^6 m^3 s^{-1}).

Southern	Northern	Western	Eastern
		Western Atlantic domain	
0.0	0.0	−10.0, south of 22.5°N 30.0, north of 22.5°N	−40.0, south of 27°N −10.0, between 27° and 38°N 100.0, between 38° and 40.5°N 0.0, between 40.5° and 41°N −30.0, between 41° and 43°N 0.0, north of 43°N
		Gulf of Mexico domain	
15.0 west of 84.6°W 0.0 east of 84.6°W	−29.0	none	−15.0, south of 20°N 0.0, between 20° and 28°N 1.0, north of 28°N

COADS wind stress. Since available wind observations are rather limited operationally, a scheme was utilized in which the hurricane's axisymmetric surface wind field was generated using the National Hurricane Center storm message file containing the information on the storm position, maximum winds, and the radii of maximum, 26 m s^{-1}, and 18 m s^{-1} winds. The asymmetry of wind speed associated with the hurricane movement was included by adding an additional vector wind $U_h/2$ (U_h is the hurricane translation speed), consistent with the recommendations of NOAA (1979). The surface stress was calculated using the usual bulk transfer formula with the drag coefficient from Large and Pond (1981). The wind empirical model was successfully tested (Ginis et al. 1996) for ocean response during Hurricane Gilbert (1988) using airborne field observations (Shay et al. 1992). The effect of air–sea heat exchange on the ocean response was neglected during this last step of the model initialization mainly due to the lack of meteorological data. This, however, caused a fairly small underestimation of the surface cooling produced by the storm. Previous numerical studies (Price 1981; Ginis and Dikinov 1989) indicate that the surface heat fluxes are much smaller then the heat fluxes due to vertical mixing for hurricane conditions and contribute about 10%–15% of to the total SST decrease in the cold wake.

e. Summary of experiments

All of the integrations presented in this study were extended to 72 h. Forecasts were made for two cases of Hurricane Opal (1996) and one case of Hurricane Gilbert (1988) in the Gulf of Mexico and two cases each of Hurricanes Felix (1995) and Fran (1996) in the western Atlantic. In order to clarify the impact of the ocean response on the storm's behavior, comparisons were made with the uncoupled operational forecasts that were run from the original NCEP SST analysis. Two additional supplemental experiments were also performed for Hurricanes Opal and Felix. In the first, a coupled forecast was run starting from the NCEP SST field that did not contain the cold wake that was generated during the fourth step of the ocean initialization. In the second of the supplemental experiments, the uncoupled experiment was run with the NCEP SST field modified by the initial cold wake. These experiments were performed to evaluate how much of the changes in storm intensity observed in the coupled experiments resulted from addition of the initial cold wake generated during the ocean initialization. In order to evaluate how much the sensitivity of the GFDL hurricane model's response to the ocean coupling was due to the model's cumulus parameterization scheme, additional coupled and uncoupled experiments were made for one case of Hurricane Opal, in which either the current parametrization was replaced by a scheme developed by Emanuel and Živković-Rothman (1999) or there was no parameterization of convection in the innermost grid. Finally, one additional set of coupled and uncoupled experiments were run for Fran, in which Edouard's cold wake was also generated during the fourth step of the ocean initialization, by imposing the hurricane wind forcing from Edouard starting five days before the start of Fran's forecast. This was done since Edouard's cold wake was virtually absent from the NCEP SST analysis that was used for the operational forecasts of Fran.

3. Experimental results

In this section, the numerical results will be presented. Discussion in sections 3a and 3b will focus on Hurricanes Gilbert (1988) and Opal (1995) in the Gulf of Mexico, with results for two Atlantic storms, Hurricanes Felix and Fran, presented in sections 3c and 3d, respectively. Finally, the results of 163 additional forecasts during the 1995–98 hurricane seasons will be summarized in section 3e. Most of the discussion will focus on changes in storm intensity measured by the storm's minimum sea level pressure. Changes in the distribution of evaporation and equivalent potential temperature due to the ocean coupling will also be shown. In all of the following discussions, the uncoupled forecasts run without a cold wake imposed during the ocean initialization will be referred to as the operational forecast, since these were the forecasts that were available to the National Weather Service operationally.

a. Hurricane Gilbert (1988)

The first forecast was made for Hurricane Gilbert (initial time of 1200 UTC 14 September 1988) just prior to its landfall on the Yucatan Peninsula. Hurricane Gilbert was a very large and intense storm as it moved across the western Caribbean Sea with a cyclonic circulation that extended over 1000 km (Bender et al. 1993b). After crossing the Yucatan Peninsula the hurricane continued on a west-northwest track over the central Gulf, making landfall again on the coast of western Mexico 60 h later.

During Gilbert's passage over the Gulf of Mexico, the ocean response was extensively measured using current and temperature observations acquired from the deployment of airborne expendable current profilers and airborne expendable bathythermographs from the NOAA WP-3Ds in the western Gulf of Mexico from 14 to 19 September 1988 (Shay et al. 1992). This experiment provided observations of the current and temperature structure before the hurricane and one and three days following the storm passage. The observations indicated the presence of a warm-core eddy northeast of the Gilbert track that formed from a cutoff meander of the Loop Current. The presence of a warm-core eddy may potentially have a significant impact on the dynamics of air–sea interaction in hurricanes and therefore should be taken into account for realistic simulations.

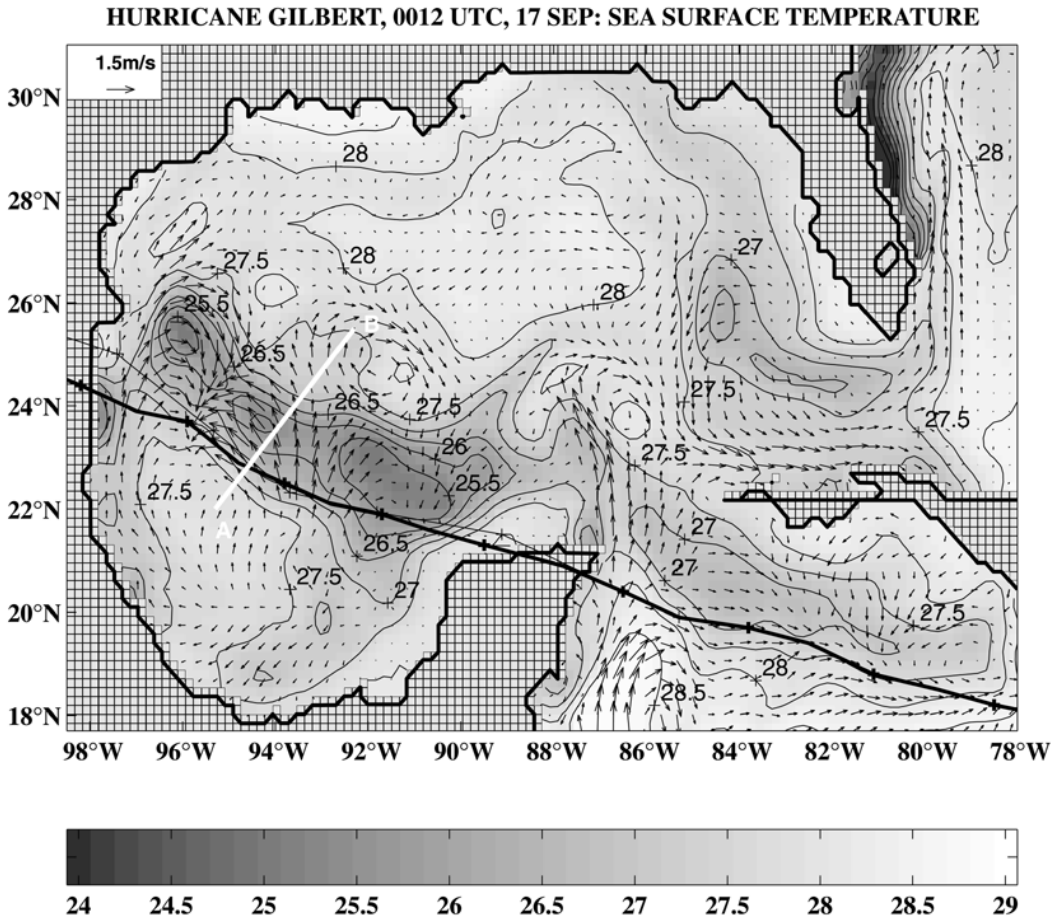

FIG. 3. The SST distribution (°C) and ocean surface currents at 72 h for the coupled experiment for Hurricane Gilbert (1200 UTC 14 Sep initial time). The contour interval is 1°C with the lower SSTs indicated by the darker shading. The observed and the 72-h forecasted tracks are shown by a thick and thin solid line, respectively, with the observed and forecasted positions at 12-h intervals indicated by crosses. The line AB indicates the cross section plotted in Fig. 4.

The observed eddy could not be initialized using only the historic data or real-time NCEP SST analysis. Therefore it was assimilated after completion of the third step of the ocean initialization. The temperature fields for the eddy with high horizontal (10 km) and vertical (10 m) resolutions and the coordinates of the eddy center during the passage of Gilbert were provided by L. Shay (University of Miami). The realistic eddy consists of both symmetric and asymmetric components. Only the symmetric components of temperature and velocity fields of the eddy were generated. The symmetric component of the temperature field was obtained by circular averaging the observed temperatures around the eddy center. This temperature field was then used to spin up the eddy currents using an idealized diagnostic (fixed temperature) model run with the same model resolution and physics as used in the prediction. During the eddy spinup, the temperatures outside the eddy were uniform and equal to the temperatures at the 250-km radial distance from the center. This integration proceeded until a balanced state was reached. Since the currents outside of the eddy were zero, the merging with the large-scale fields was simply performed by adding the eddy currents and the temperature deviations from the uniform values. The ocean model was then run for another 10 days for dynamical adjustment between the eddy and surrounding environment, keeping the SST fixed. The resulting prestorm SSTs and surface currents in the ocean model are shown in Fig. 2. The Loop Current is well represented in the model but its structure is not sharpened enough due to the coarse resolution of the climatological fields used for the model initialization. Note that prestorm SSTs of 28.4°–28.7°C were fairly uniform over the Gulf and Caribbean Sea before Gilbert's arrival. The SST field displays no apparent signature of the warm eddy since its structure is mainly confined to the thermocline. Very weak signatures of warm-core eddies at the surface are typical for summertime SST analyses in the Gulf of Mexico due to strong solar heating.

The track forecast made by the model was exceptionally accurate (Fig. 3), with a 48-h forecast error of only 40 km. Gilbert produced a cold wake at the sea

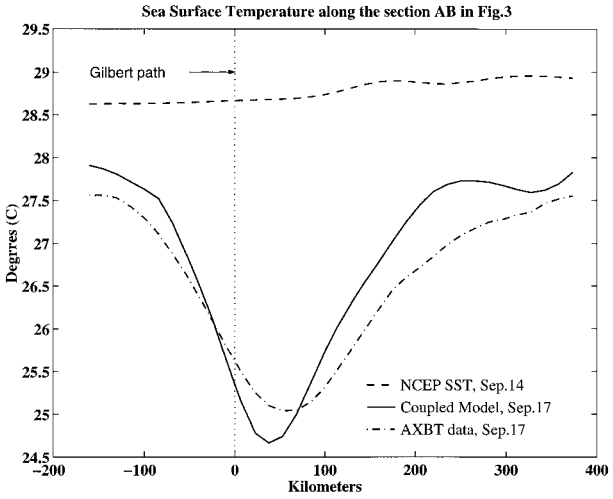

FIG. 4. SST distribution from the coupled experiment (solid line) along section AB in Fig. 3, compared with objectively analyzed AXBT data (dashed–dotted line) from Shay et al. (1992) on 17 Sep 1987. Initial prestorm surface temperature (dashed line) from the NCEP SST global analysis is shown as well.

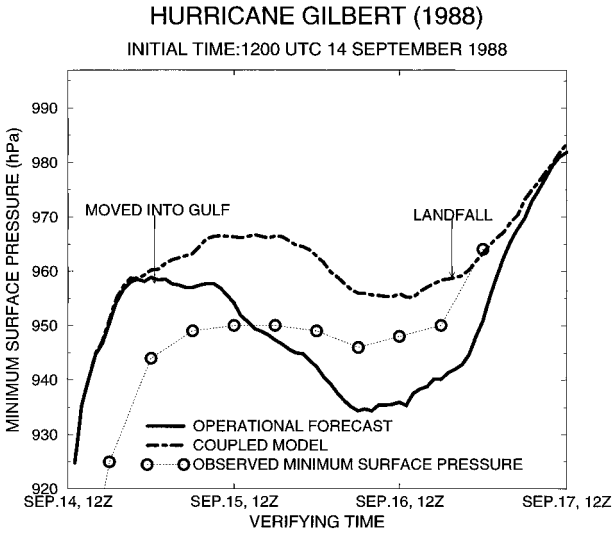

FIG. 5. Time series of minimum sea level pressure for the operational forecast (solid line) and coupled experiment (dotted–dashed line) compared to observed values (thin dotted line, circles indicating values every 6 h) for the forecast of Hurricane Gilbert.

surface over a broad area 100–200 km wide, with a pronounced rightward bias in the SST decrease with respect to the storm track. This rightward asymmetry is well established from previous observations and numerical studies (e.g., Black 1983; Chang and Anthes 1978) and is correlated with the asymmetry in the mixed layer currents and the mixed layer deepening underneath the storm. Maximum cooling occurred over the continental slope and the deep water areas in the middle of the Gulf where the mixed layer is shallower and the thermocline stratification is steeper. The maximum SST decrease exceeded 3.5°C at some places as the SSTs decreased to a minimum of 25.2°C. The effect of the warm-core eddy on the hurricane-induced cooling was generally insignificant in this case, mainly due to the large distance (about 250 km) from its center to the storm track. The pattern of SST decrease demonstrated very different oceanic responses in the Gulf and Caribbean Sea. Despite its extreme intensity in the northwestern Caribbean, Gilbert generated relatively small SST decrease there (maximum of 1.7°C) mainly due to the significantly deeper initial upper mixed layer of about 70 m. Moreover, the SST decrease was also rather insignificant over the shallow continental shelf surrounding the Yucatan Peninsula and near the coast of eastern Mexico, where the vertical temperature gradients are weak.

The magnitude and the pattern of SST decrease produced by the coupled model was generally in good agreement with the observations (Shay et al. 1992). For example, Fig. 4 shows the comparison of the simulated SST and objectively analyzed observed fields from Shay et al. (1998a) along the section AB in Fig. 3. The field experiment during Gilbert also provided the measurements of currents before, during, and after the storm. The detailed comparisons between the model and observed data is a subject of future studies. We only note here general consistency, especially in the region of strong wind-driven currents near the storm track and in the vicinity of the warm-core eddy. For example, the maximum of the mixed layer currents that diverged from the storm track as part of the near-inertial rotation was about 1.2–1.4 m s^{-1} (Fig. 3), which agreed well with the observations (Shay et al. 1998a).

At the start of the forecast, the hurricane was near maximum intensity with a minimum sea level pressure of 892 hPa and maximum low-level winds of nearly 72 m s^{-1}. The observed storm was about 35 hPa deeper than the model storm (Fig. 5), since the model resolution was insufficient to reproduce the storm's extreme intensity. Once the storm made landfall on the Yucatan Peninsula and began weakening, the observed and model storm filled to 949 hPa and 959 hPa, respectively. After moving into the Gulf and prior to the final landfall on the eastern Mexican coast 48 h later, Hurricane Gilbert underwent only very slight reintensification (4 hPa) to 946 hPa. In contrast, in the operational forecast without ocean coupling, the storm began to gradually reintensify over the warm open Gulf waters, deepening 25 hPa to 934 hPa during the next two days. With the coupling included the reintensification was much smaller and closer to the observed rate, with about a 10-hPa deepening. Although the storm in the coupled model remained somewhat weaker than observed during this period, the general tendency of the minimum sea level pressure was improved compared to the operational model. This suggests that the large SST decrease produced by Gilbert in the Gulf of Mexico was likely one

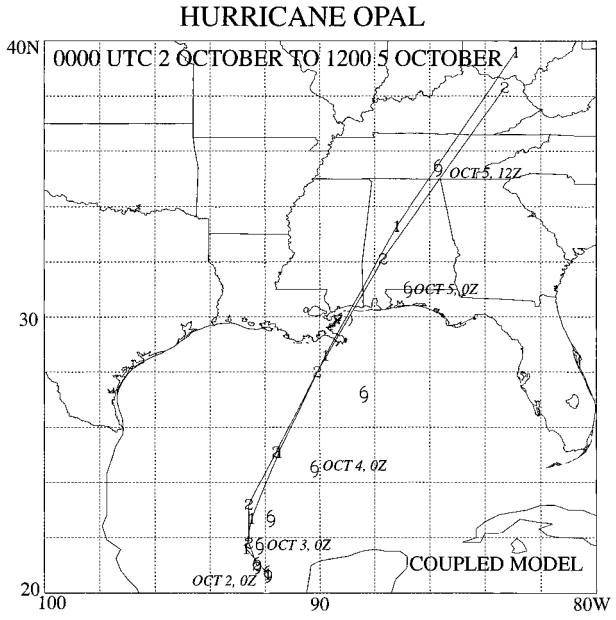

FIG. 6. The 72-h storm tracks (thin lines) for the two forecasts of Hurricane Opal made by the coupled model starting at 0000 and 1200 UTC 2 Oct. The storm positions at 12-h intervals are indicated by the symbols 1 and 2 for the forecasts starting at 0000 and 1200, respectively. The observed positions at 12-h intervals are indicated by the storm symbols.

of the majors factor that prevented significant reintensification of the hurricane.

b. Hurricane Opal (1995)

The second case studied also involved an intense hurricane (Hurricane Opal) that occurred in early October of 1995. After slowly moving west of the Yucatan, Opal intensified to tropical storm strength, as it continued to drift in the southern Gulf of Mexico for several days before turning north and eventually making landfall near Pensacola, Florida (Fig. 6). Two sets of forecasts were made, starting at 0000 and 1200 UTC 2 October prior to the storm's northward turn. The minimum sea level pressure of Opal at the start of the two forecasts was 985 and 972 hPa, respectively, with maximum surface winds of 31 and 33 m s^{-1}. Opal initially moved slowly (220 km) during the first 36-h period from 0000 UTC 2 October to 1200 UTC 3 October. Due to the slow storm motion, both of the forecasts with the ocean coupling produced a large SST decrease in the region just northwest of the Yucatan. The forecast starting at 0000 UTC 2 October produced a maximum cooling of 4.5°–4.7°C (Fig. 7). This exceptionally strong cooling is consistent with the very slow movement of Opal and shallow prestorm mixed layer depths of about 20–30 m as the area of maximum cooling located around 21.8°N, 92°W was exposed to continuous hurricane forcing over more than three days, from 30 September to 3 October. The large ocean response during this time period was significantly greater than found for the majority of Atlantic storms. However, slow moving ($<$2.5 m s^{-1}) or looping storms in the Atlantic basin occur only about 20% and 10% of the time, respectively, in the 20°–30° latitudinal belt (Xu and Gray 1982). Moving much faster over the open Gulf of Mexico during the next two days, the model storm generated cooling of 1.5°–1.7°C over a 150–250-km-wide area to the right of the track. The amplitude and spatial extent of the SST anomalies in the model are consistent with the satellite AVHRR observations (P. Black, NOAA/AOML Hurricane Research Division, 1997, personal communication).

As mentioned in section 2, since there was no detectable cold wake in the NCEP analysis, the SST distributions for the coupled experiments were modified by introducing an initial cold wake during the ocean model initialization to give a more realistic initial field. Before presenting the coupled experiment results, it is important to isolate how much of the changes in storm intensity resulted from the effect of the ocean coupling and how much resulted from addition of the initial cold wake. To address this question, the results from the coupled experiment without the initial wake and results from the uncoupled experiments with the initial cold wake are included in the following discussion.

As Opal slowly drifted north during the first day and a half and was impacted by the low SSTs from the cold wake, the minimum sea level pressure deepened only about 15 hPa, to 970 hPa (Fig. 8). In contrast, in the operational forecast (solid line), the model storm began to rapidly intensify with the predicted sea level pressure starting from the 0000 and 1200 UTC initial times, dropping to 927 hPa and 931 hPa, respectively, by 1200 UTC 3 October (58- and 41-hPa deepening), compared to the observed pressure of 970 hPa. In the experiments with both the coupling and the initial cold wake included (dashed–dotted line), the storm's intensity was much better reproduced compared to the operational forecast, and the forecasted minimum sea level pressures at 1200 UTC 3 October were 960 hPa and 973 hPa, respectively, starting from the 0000 and 1200 UTC initial times. Note, that with the inclusion of the initial wake from the beginning, even without the ocean coupling (dashed line) the rapid intensification was considerably reduced compared to the operational forecast, particularly in the forecast starting at 1200 UTC where the storm propagation speed was somewhat slower and the storm remained near the region of the largest SST decrease longer. Starting from this time period, during the first 24 h the coupled model experiments without the initial cold wake (thin solid line) had a similar intensity as the uncoupled experiment with the cold wake. This was because the SSTs in the coupled experiment rapidly decreased underneath the slow moving storm from the beginning of the coupled forecast. As discussed previously, shallow mixed layer depths and strong stratification of the thermocline waters in the southern Gulf create very favorable conditions for rapid cooling of the sea surface by

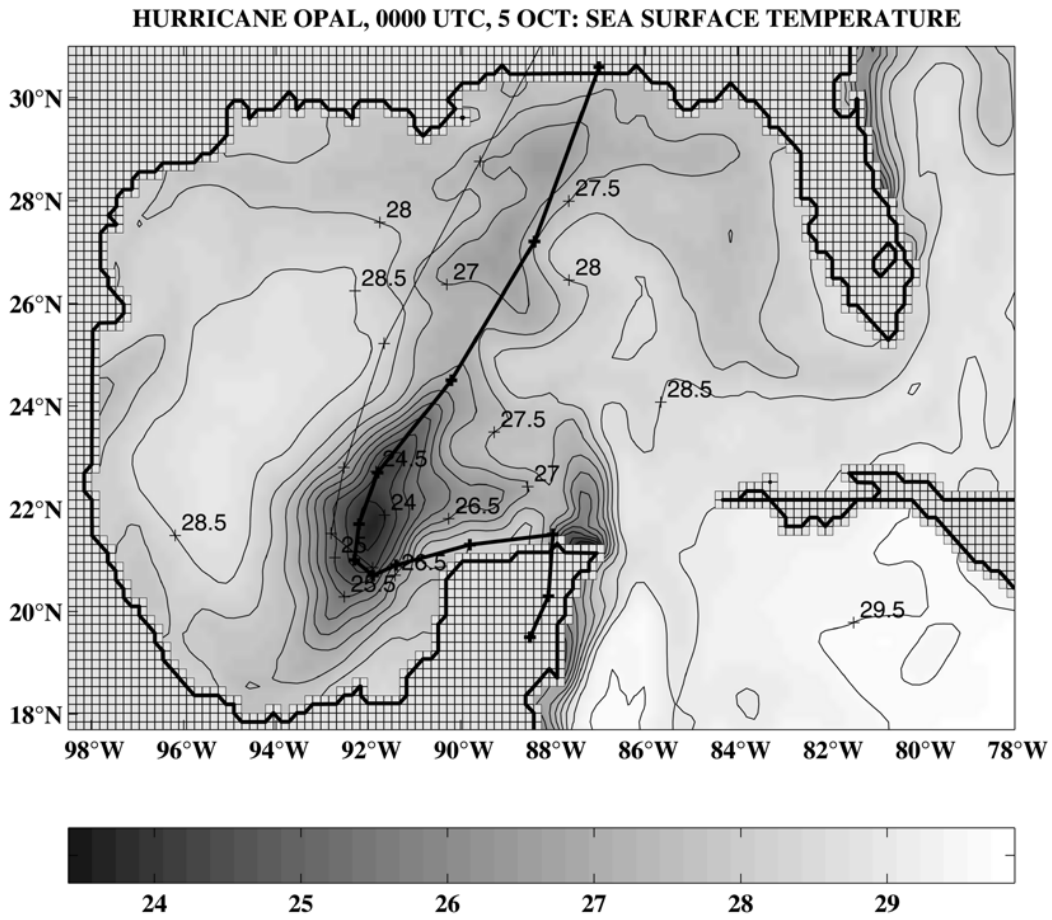

FIG. 7. The SST distribution (°C) at 72 h for the coupled experiment for Hurricane Opal (0000 UTC 2 Oct initial time). The contour interval is 0.5°C with the lower SSTs indicated by the darker shading. The observed track starting from the 1200 UTC 29 Sep position and the 72-h forecasted track are shown by a thick and a thin solid line, with the observed and forecasted positions at 12-h intervals indicated by crosses.

strong hurricane-induced turbulent mixing. In the integrations beginning at the 0000 UTC initial time, the difference in intensity was small between the two coupled experiments run with and without the initial cold wake. This indicates that despite the slow movement of Opal, inclusion of the initial wake was still of secondary importance compared to the effect of the coupling itself.

On 3 October, as Opal accelerated to the north it rapidly strengthened. In the coupled forecast beginning at 1200 UTC 2 October in which the storm speed was well forecasted, the storm began to intensify after 1200 UTC 3 October, similar to the observed storm although at a smaller rate. This suggests that the main reason for Opal's rapid intensification was due to the storm's acceleration from 2–3 m s^{-1} to about 10 m s^{-1} over a 12-h period. In the first forecast where the model storm moved north too quickly, the intensification began somewhat earlier than observed and was too rapid. These results are consistent with previous idealized studies and observational results (e.g., Chang and Anthes 1978; Black 1983) indicating that the SST decrease is strongly correlated with the storm's translational speed.

Up to the time the model storm crossed the coast, the deepening continued. Obviously after landfall the model storm rapidly decayed while the observed storm continued to deepen up to about 8 h before landfall. Even if the storm motion had been accurately forecasted, the rapid deepening of Opal during 4 October would probably not have been reproduced by the present hurricane model in part due to the insufficient $\frac{1}{6}^{\circ}$ model resolution that could not adequately resolve the inner eyewall structure. With a higher-resolution coupled model it is likely that the intensity of Opal during its most intense period will be better simulated. Another likely reason for underprediction is that the present experiments did not take into account a warm ocean eddy in the Gulf of Mexico, which was detected by altimeter data during the poststorm analysis (Shay et al. 1998b). According to the observations, during the deepening phase, Opal moved over a warm ocean eddy located just to the right of the hurricane path and centered at about 25°N, 88°W.

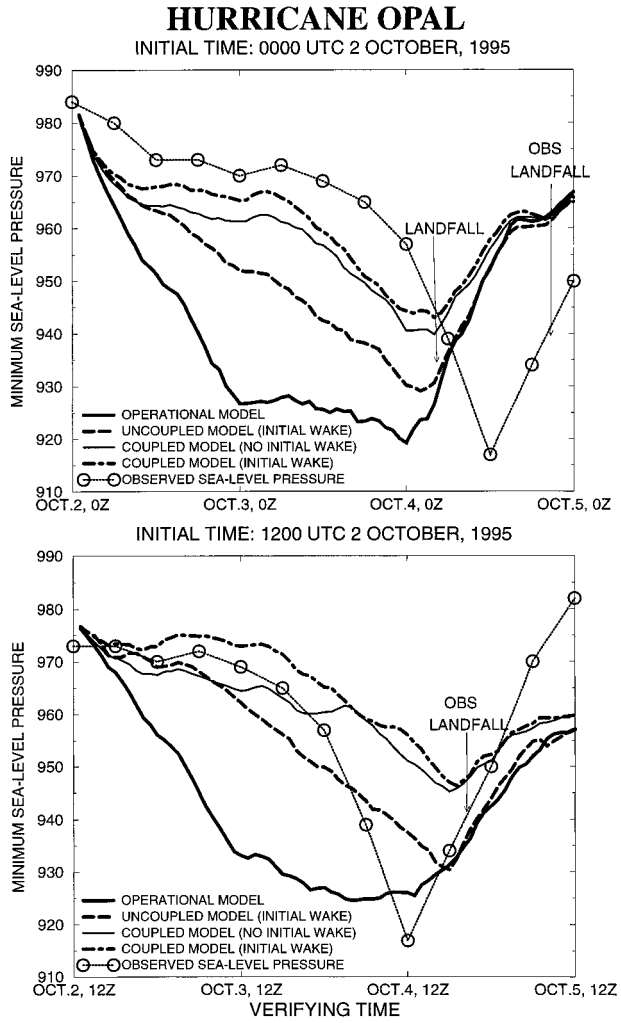

FIG. 8. Time series of minimum sea level pressure for the operational forecast (uncoupled model without the initial cold wake, thick solid line), the uncoupled experiment with (dashed line) the initial cold wake, and the coupled experiments without (thin solid line) and with (dotted–dashed line) the initial cold wake for the forecasts of Hurricane Opal beginning at the 0000 and 1200 UTC 2 Oct initial time. The observed values (thin dotted line, circles indicating values every 6 h) are also plotted for comparison.

The hurricane-induced ocean cooling could have been substantially reduced over the eddy due to increased heat content in the upper ocean. Since the simulated tracks of Opal in the present study moved the storm about 100 km to the west of the eddy, its impact on the storm intensity could not be addressed adequately and therefore awaits further investigation.

In order to examine the mechanisms contributing to the differences in storm intensity for these four experiments, the accumulated evaporation is presented next. Figure 9 indicates the dramatic effect the cold wake had on the accumulated evaporation throughout the period up to landfall. During the first 36 h, as the storm moved north, in the operational model the rather slow movement produced very large values of accumulated evaporation on both sides of the track with the largest amount ($\sim$3.8 cm) to the right. Since the region of maximum evaporation was located very close to the region of largest SST decrease, the evaporation was reduced by 65% to about 1.7 cm in this region in both coupled experiments (Fig. 9, bottom), and the region of largest accumulated evaporation was located to the left of the track. During the first 24 h, the addition of the cold wake in the coupled experiment further reduced the accumulated evaporation near the storm center about 25% compared to the coupled forecast run without the cold wake. Note that in the uncoupled experiment the addition of the initial cold wake caused the accumulated evaporation to become significantly less even up to the point of landfall, as the storm remained weaker throughout the forecast (Fig. 8). This contributed to the large reduction in the rapid intensification seen in Fig. 8.

Assuming neutrality to slantwise convection, Emanuel (1986) derived a simple linear relationship between the differences in the equivalent potential temperature $\Delta\theta_e$ and the sea level pressure Δp_* between the storm center and the outer storm periphery:

$$\Delta p_* = -(3.3)\Delta\theta_e. \tag{3.1}$$

Table 4 summarizes the values of $\Delta\theta_e$, Δp_*, and their ratio at 36 h, for all of the experiments in the Gulf of Mexico, computed between the storm center and the circular average at 250-km radius surrounding the storm. They demonstrate the direct impact on the storm intensity from the decreased boundary layer moist static energy resulting from the cold wake. Even at 36 h the influence of the cold wake was still evident east of the center well away from the initial wake (Fig. 10, right top). This resulted in a decrease of nearly 4° in the distribution of the equivalent potential temperature compared to the operational forecast. By 36 h the distribution of the equivalent potential temperature was similar in both of the coupled experiments, resulting in a similar storm intensity (Fig. 8). For the two coupled experiments of Opal starting at 1200 UTC, the values of $\Delta\theta_e$ were 11.2 and 11.3 K, which were well correlated with the surface pressure difference Δp_* of 41 and 39 hPa, respectively. The combined effect of the ocean coupling and slow storm movement on the supply of moist static energy is very apparent as the equivalent potential temperature east of the storm center was about 8 K lower in both coupled experiments compared to the operational forecast (Fig. 10), which had values of 17.5 K and 70 hPa for $\Delta\theta_e$ and Δp_* (Table 4).

The ratio $\Delta p_*/\Delta\theta_e$ varied somewhat in time, and between storms and experiments, suggesting the importance of factors other than $\Delta\theta_e$ on the storm intensity at any given time. Nevertheless the ratio averaged 3.6 for the 10 experiments, which was in fairly good agreement with the estimates of Emanuel (1986). This suggests that the relationship obtained in these experiments between the storm intensity and the changes in the SST

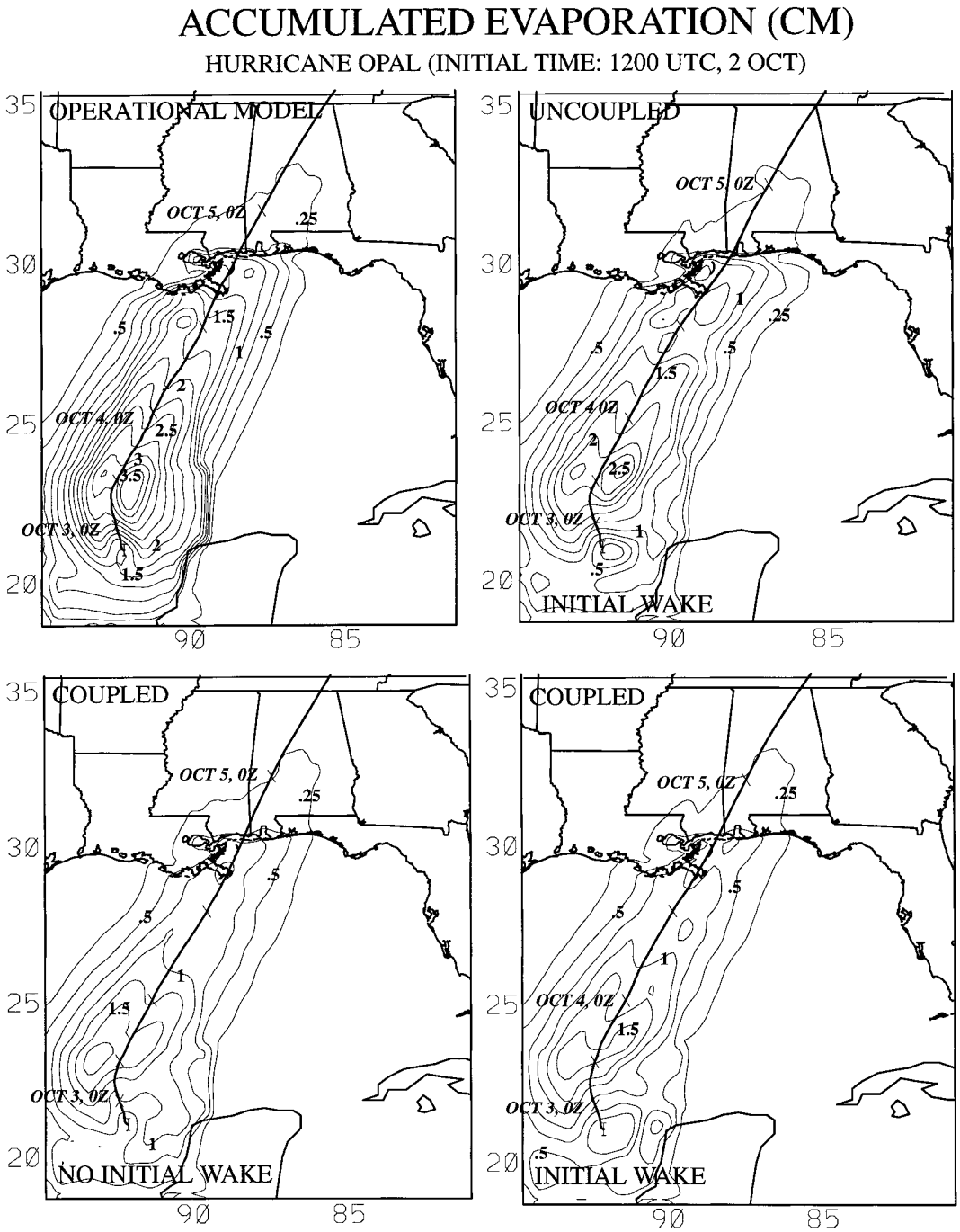

FIG. 9. Distribution of evaporation (cm) for the operational forecast (uncoupled model without the initial cold wake; top, left), the uncoupled experiment with the initial wake (top, right), and the coupled experiments without (bottom, left) and with (bottom, right) the initial wake accumulated during passage of Hurricane Opal for the forecasts starting at 1200 UTC 2 Oct. The contour interval is 0.25 cm with the forecasted track indicated by the thick solid line.

from the ocean–atmospheric interaction were reasonable.

The sensitivity of the GFDL hurricane model's response to the ocean coupling due to changes in the cumulus parameterization scheme was also evaluated. To address this issue two additional sets of coupled and uncoupled experiments were performed. In the first set of experiments the current parameterization was replaced by a scheme developed by Emanuel and Živković-Rothman (1999) in which the effects of entrain-

TABLE 4. Difference in equivalent potential temperature and sea level pressure between the storm center and the storm periphery at 36 h; for all experiments in the Gulf of Mexico.

Hurricane	Expt	$\Delta\theta_e$ (K)	Δp_* (hPa)	$\frac{\Delta p_*}{\Delta\theta_e}$ (hPa K^{-1})
(1200 UTC 14 Sept 1988)				
Gilbert	Operational forecast	16.4	57	3.5
Gilbert	Coupled, initial wake	10.7	37	3.5
(0000 UTC 2 Oct 1995)				
Opal	Operational forecast	15.8	66	4.2
Opal	Not coupled, initial wake	11.7	43	3.6
Opal	Coupled, no initial wake	9.6	34	3.5
Opal	Coupled, initial wake	9.4	29	3.1
(1200 UTC 2 Oct 1995)				
Opal	Operational forecast	17.5	70	4.0
Opal	Not coupled, initial wake	14.8	55	3.7
Opal	Coupled, no initial wake	11.2	41	3.7
Opal	Coupled, initial wake	11.3	39	3.5
	Average ratio for Gulf of Mexico			3.6
	Ratio from Emanuel (1986)			3.3

ment, cloud microphysical processes, and convective downdrafts are estimated. In the second set of experiments, there was no parameterization of convection in the innermost grid and the precipitation was produced entirely by large-scale condensation on the resolvable scale. In this set of experiments the convective parameterization was retained in the outer nests, since the precipitation processes could not be resolved in a reasonable way in the coarser resolution without cumulus parameterization. Figure 11 indicates that in each of the sets of experiments, the ocean coupling had considerable impact on the storm intensity. During the first 36 h, the storm rapidly intensified in all three forecasts run without the ocean coupling, although the rate of intensification varied in each experiment. With the parameterization of Emanuel and Živković-Rothman (1999), the storm tended to exhibit the largest sensitivity to the ocean coupling, since the storm showed only slight strengthening during the 12-h period prior to the model storm's landfall. Nevertheless, in each case, the ocean coupling greatly reduced the model's strong positive intensity bias exhibited during the first part of the forecast when the storm was slowly drifting north. The sensitivity of storm intensity to the type of cumulus parameterization used in the GFDL model remains an interesting topic that is now currently being investigated for other cases.

A final consideration in this section is the sensitivity of the hurricane response to the ocean coupling as a function of the vertical resolution of the GFDL model. A new version of the GFDL hurricane model has recently begun to be tested in which the number of vertical sigma levels was increased from 18 to 42 levels. The new vertical configuration corresponds to the T170 global model that was made operational at NCEP in 1998 (Derber et al. 1998). In this higher-resolution model, the number of vertical levels in the boundary layer was increased from four to eight. Preliminary tests with this model indicate that some of the simulated storms tend to be slightly more intense. For example, for the uncoupled forecast starting from the 0000 UTC 2 October initial time, the minimum sea level pressure in the 18-level model averaged 925 hPa during the second day of the forecast compared to 917 hPa for the 42-level model (not shown). However, the model's response to the ocean coupling remained very similar, despite the increased resolution and storm intensity. For example, during the same forecast period, the average differences in the minimum sea level pressure between the coupled and uncoupled forecasts were 33 hPa and 31 hPa, respectively, for the 18- and 42-level models. The impact of both vertical and horizontal resolutions on the GFDL hurricane model is currently being carefully evaluated. Nevertheless, these preliminary results have demonstrated that the sensitivity of the GFDL model to the effect of the ocean coupling, which is the primary focus of this study, was not dependent on the particular convective parameterization or the model's vertical resolution.

In summary, in these forecasts of Opal, the ocean coupling had an important effect on the storm intensity especially during the early period of the forecast, as the storm drifted north. Furthermore, inclusion of both the initial cold wake and the ocean coupling was found to be important to reduce the large positive intensity bias during the first part of the forecast when the storm was greatly impacted by the reduced supply of moist static energy. Although the effect of the initial cold wake was still of secondary importance compared to the effect of the ocean coupling, comparisons of the experiments run with and without the initial wake suggest the importance of accurate representation of the SST in the initial analysis for the prediction of storm intensity.

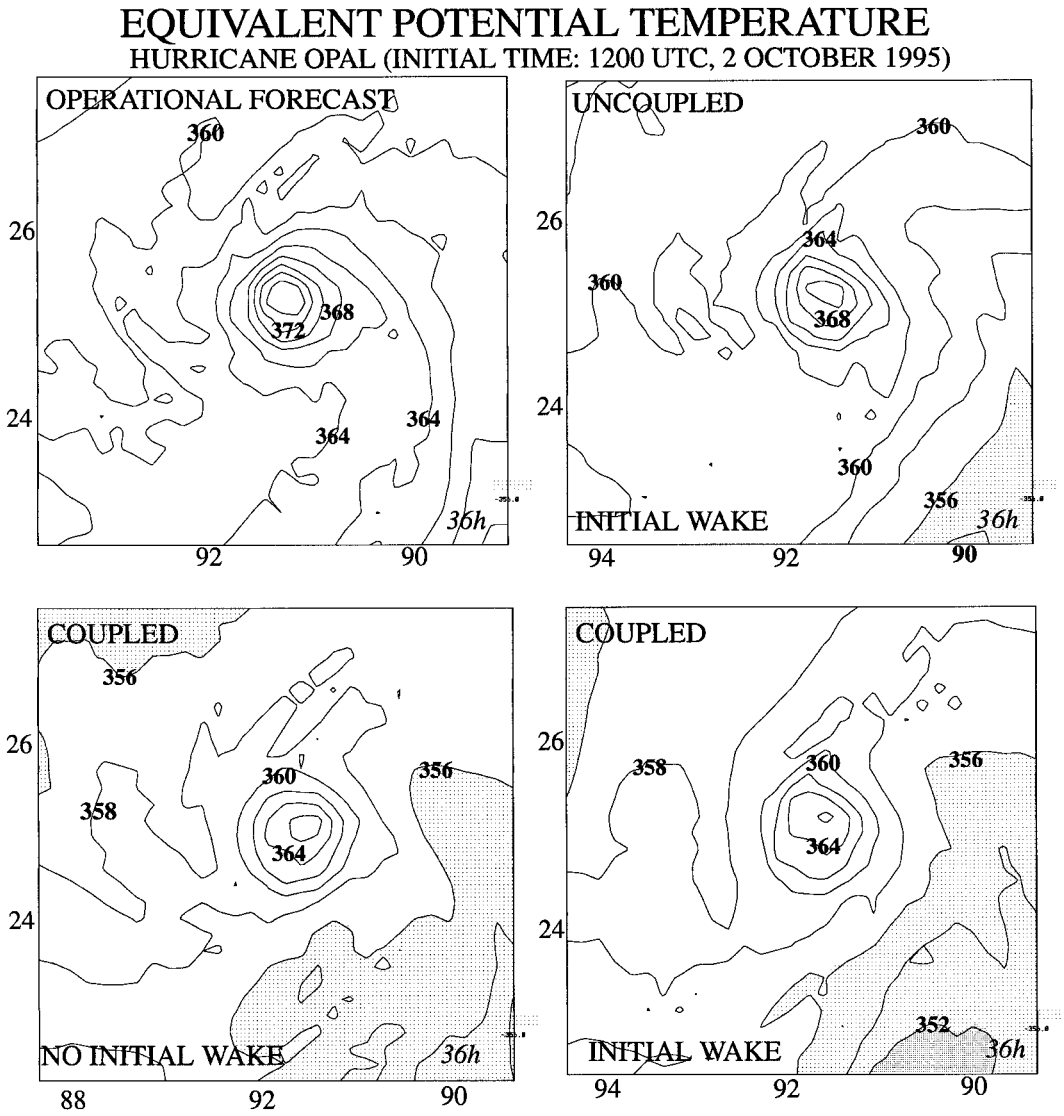

FIG. 10. The 36 h distribution of the equivalent potential temperature (K) at model level 18 (σ = 0.995, ~40 m height) for the operational forecast (uncoupled model without the initial cold wake, top, left), the uncoupled experiment with the initial wake (top, right), and the coupled experiments without (bottom, left) and with (bottom, right) the initial wake (1200 UTC 2 Oct initial time) for Hurricane Opal. The contour interval is 2 K with values less than 356 K and 352 K indicated by light and thick shading, respectively.

c. Hurricane Felix (1995)

In the next set of experiments, two forecasts of Hurricane Felix were selected. Hurricane Felix was the first major hurricane of the very active 1995 hurricane season. The system initially formed near the Cape Verde Islands reaching tropical storm strength on 8 August, steadily moving west-northwest during the next four days as it intensified. It reached maximum intensity on 0000 UTC 13 August, with maximum winds of 59 m s^{-1} and minimum sea level pressure of 930 hPa. Felix turned to the north-northwest on 13 August (Fig. 12) and then almost due north, weakening 35 hPa during the next two days. The first forecast began on 0000 UTC 13 August, at the time of maximum intensity, with the second forecast beginning 24 h later. Both the track and storm speed were well predicted in both forecasts (Fig. 12). During this period, the relatively slow movement of Felix (~3.5–4.0 m s^{-1}) caused a very large cold wake to form to the right of the storm track (Fig. 13). In the forecast starting from the 0000 UTC 14 August initial time, the maximum SST decrease was about 5°C (minimum of 23°C) centered at about 26°N.

During 15 August, the center of Hurricane Felix passed 225 km southwest of the island of Bermuda, also passing within 65 km of the Bermuda Testbed Mooring located at 31°43.4′N and 64°10.1′W (Dickey et al.

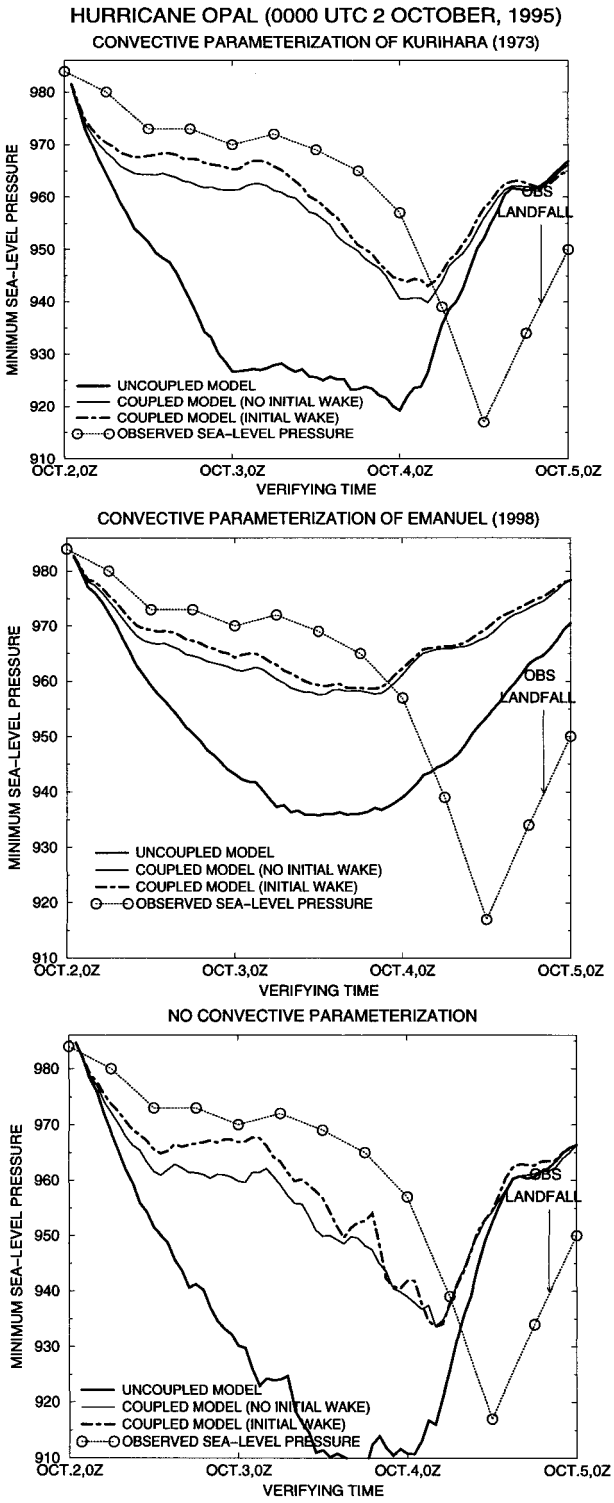

FIG. 11. Time series of minimum sea level pressure for the uncoupled forecast without the initial wake (solid line) and coupled experiment with (dotted–dashed line) and without (thin solid line) the wake compared to observed values (dotted line, circles indicate values every 6 h) for one of the forecasts of Hurricane Opal run with the current parameterization scheme, the parameterization scheme of Emanuel and Živković-Rothman (1999), and with no convective parameterization in the inner nest.

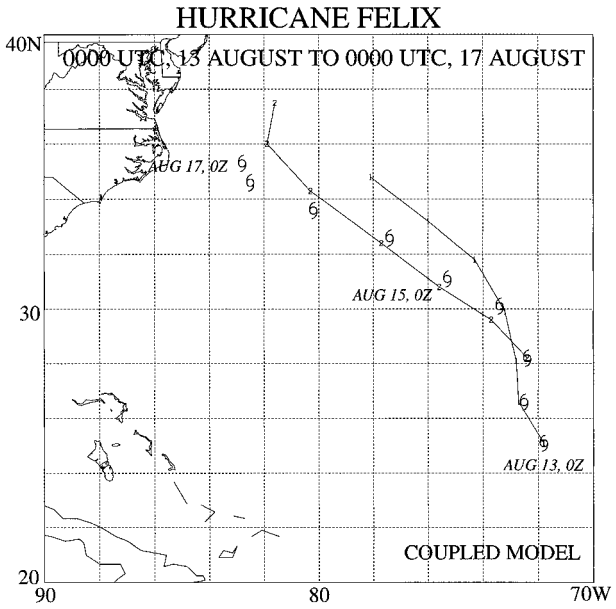

FIG. 12. The 72-h storm tracks (thin lines) for the two forecasts of Hurricane Felix made by the coupled model starting at 0000 UTC 13 and 14 Aug. The storm positions at 12-h intervals are indicated by the symbols 1 and 2 for the forecasts starting on 13 and 14, Aug, respectively. The observed positions at 12-h intervals are indicated by the storm symbols.

1998). Since both the track and speed of the storm were well forecasted as the storm passed this location, this provided an excellent opportunity to verify the predicted SSTs from the coupled model integration against the observed values. As Felix passed near Bermuda, a peak wind speed was measured over the testbed mooring of 37.5 m s^{-1}, which was somewhat larger than the model-predicted maximum wind of 31 m s^{-1} at that location. The storm was moving northwestward during this time, in a nearly straight-line path at about 7 m s^{-1}. The temperature at 25-m depth decreased by 3.2°–3.5°C at the mooring location (Dickey et al. 1998), which was well correlated with satellite AVHRR SST maps (Nelson 1998) that showed a swath of cool water (~3.2°–3.5°C and 400 km wide) produced by Felix. The coupled model prediction shown in Fig. 13 agreed well with these observations. The comparisons of the model- and AVHRR-derived SSTs along the 31.75°N latitude (Fig. 14) indicate that both the prestorm SSTs on 14 August and in the cold wake on 17 August were consistent with the satellite observations. However, the minimum SST predicted by the model in the cold wake was about 25.2°C, which was about 0.7°–1.0°C higher than observed. This result may be related to the differences between the actual and the model prestorm upper ocean structure. Both model simulations and observations displayed marked asymmetry of the cold wake relative to the storm track as the position of maximum cooling was biased to the right of the storm track (Figs. 13 and 14). This rightward bias was primarily related to the wind

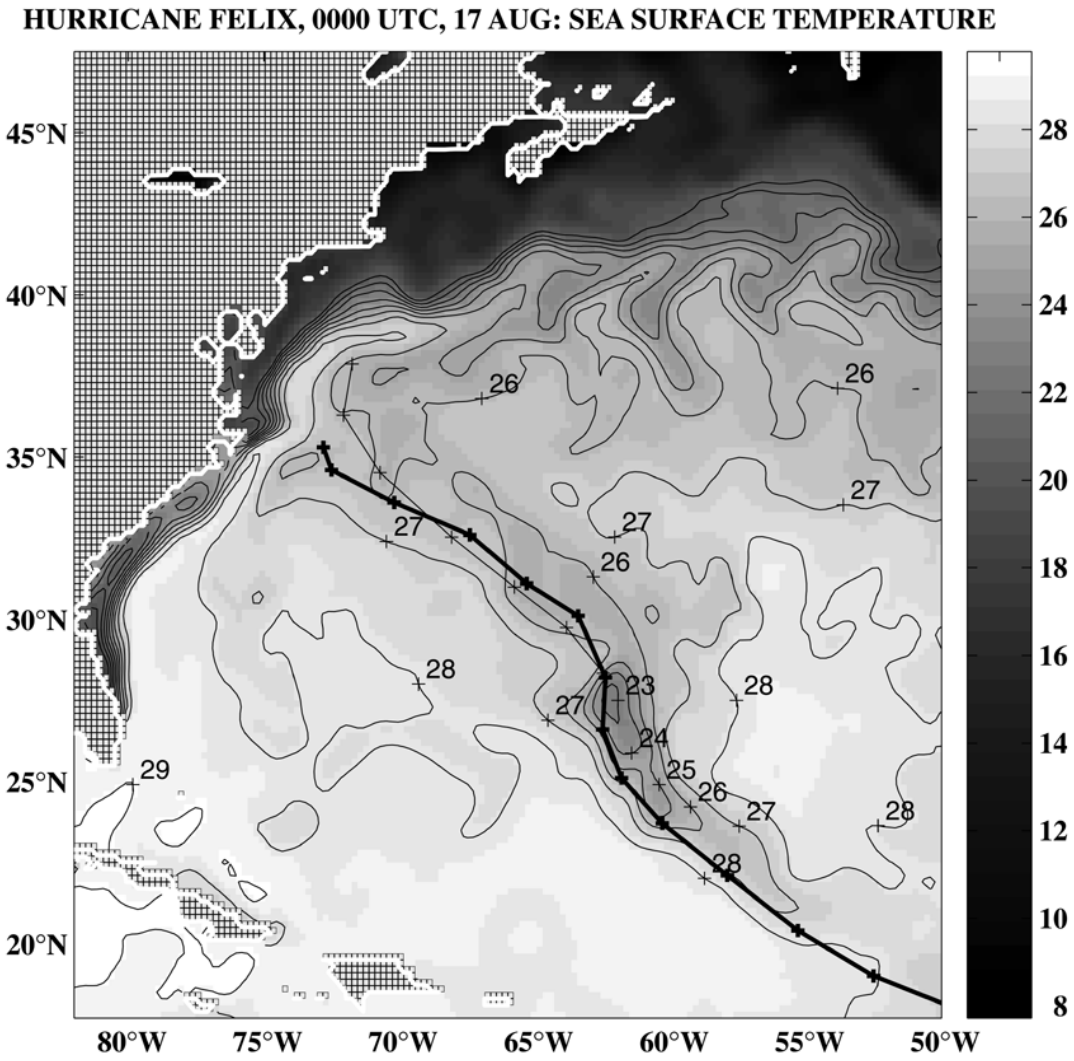

FIG. 13. The SST distribution (°C) at 72 h for the coupled experiment for Hurricane Felix (0000 UTC 14 Aug initial time). The ocean model domain for the forecasts in the west Atlantic is shown. The contour interval is 1°C with the lower SSTs indicated by the darker shading. The observed track starting from the 0000 UTC 10 Aug position and the 72-h forecasted track are shown by a thick and thin solid line, respectively, with the observed and forecasted positions at 12-h intervals indicated by crosses.

stress vector rotation, which is effectively clockwise on the right side of tracks and often in near resonance with the inertially rotating hurricane-induced surface currents (Price 1981). The level of asymmetry is therefore largely dependent on the timescale over which the ocean experiences the hurricane's wind stress. The latter is controlled by the storm's forward speed and horizontal wind structure. In Fig. 14, the position of maximum cooling in the model-simulated SSTs was displaced slightly more to right of the storm path compared to observations. Since the forward speed was predicted rather well by the coupled model, these differences may be related to the differences between the predicted and real surface winds.

The resulting change in the storm intensity is shown next (Fig. 15). The two supplemental experiments (coupled with no initial wake and uncoupled with the initial wake) were also included for both forecast times. Beyond 36 h, as the storm moved away from the initial cold wake, the differences in the storm intensity became small, especially for the first forecast, indicating that the storm intensity was no longer significantly impacted by the absence of the cold wake in the NCEP SST analysis. The 36-h distributions of the equivalent potential temperature are presented in Fig. 16 for each of the four experiments starting at 0000 UTC 13 August, and confirm that by 36 h the initial wake had little effect on the moist static energy in either the coupled or uncoupled experiments. The good correlation between $\Delta\theta_e$ and Δp_* (Table 5) demonstrates the crucial importance of the supply of the moist static energy to the storm intensity. Although the storm was moving at about 5 m

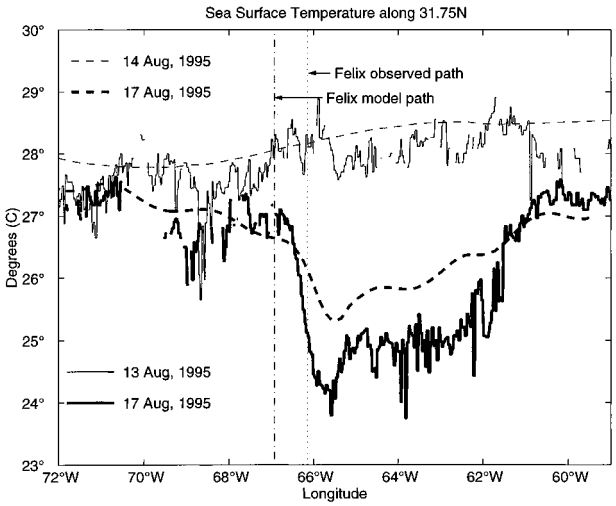

FIG. 14. Cross sections of SST (°C) along 31.75°N at the initial time of 0000 UTC 14 Aug (thin dashed line) and 72 h later (thick dashed line), predicted by the coupled model. The observed SSTs from 3-day composite satellite images of AVHRR, centered on 13 (thin solid line) and 17 Aug (thick solid line) are also shown. The longitudes where both the modeled and the observed storms crossed this latitude are indicated by the vertical lines.

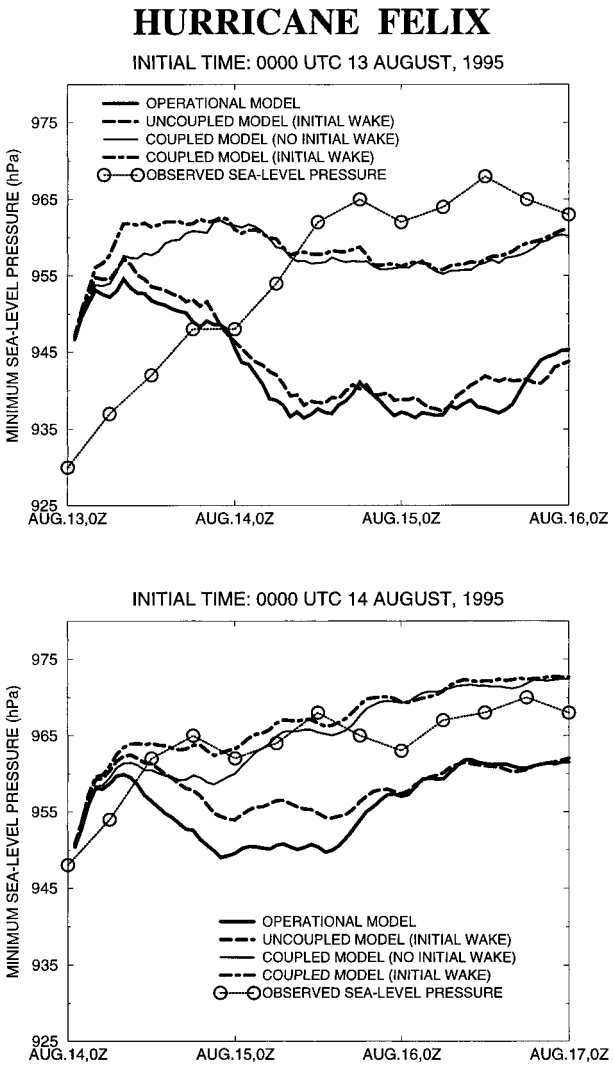

FIG. 15. Time series of minimum sea level pressure for the operational forecast (uncoupled experiment without the initial cold wake, thick solid line), the uncoupled experiment with (dashed line) the initial cold wake, and the coupled experiments without (thin solid line) and with (dotted–dashed line) the initial cold wake for the forecasts of Hurricane Felix beginning at 0000 UTC 13 and 14 Aug 1995. The observed values (thin dotted line, circles indicating values every 6 h) are also plotted for comparison.

s^{-1} and was north of the maximum SST decrease (Fig. 13) at 36 h, the coupling still produced a decrease in θ_e of nearly 6 K on the east side of the storm (Fig. 16), and $\Delta\theta_e$ in the two uncoupled experiments were 15.5 and 14.7 K compared to 8.9 K for both coupled experiments. It is interesting to note that in the forecast beginning 24 h later (0000 UTC 14 August) the ratio of $\Delta p_*/\Delta\theta_e$ was smaller (3.4 compared to 4.9 hPa K^{-1}) and was very close to the theoritical estimates of Emanuel (1986). This indicates that although the supply of moist energy is crucial in the maintenance of the storm intensity, other factors (e.g., static stability, the upper-level flow field) were important as well. This may particularly have been true as Hurricane Felix continued to move toward higher latitudes.

The model resolution could not adequately resolve the inner-core structure of Felix during its intense period and the initial minimum sea level pressure in the first forecast (Fig. 15, top) was about 17 hPa greater than observed. For both forecasts, the insufficient model resolution as well as the initialization likely contributed to the initial rapid weakening during the first 6 h, as the minimum sea level pressure filled 10 hPa even without coupling included. After a several-hour period of adjustment, in both operational forecasts the storms thereafter began to intensify during the next 24 h while the observed storm continued to weaken. This resulted in significant over intensification. By 36 h, the operational model predicted a minimum sea level pressure of 937 and 950 hPa for both experiments, compared to observed values of 962 and 968 hPa, respectively. It is uncertain how much the rapid weakening during the first 12 h would have been reduced with higher resolution leading to a more realistic intensity prediction particularly for the forecast starting at 0000 UTC 13 August. Nevertheless, during the remaining 1.5 days of the forecast, the coupled model minimum sea level pressure remained nearly constant at about 960 hPa, in good agreement with the observed storm intensity and intensity change. In the coupled experiment starting one day later, the intensity change was again well forecasted.

In summary, the results for Hurricane Felix have shown that the large SST decrease that occurred as the storm's forward speed slowed down (Fig. 13) probably played an important role in the rapid storm weakening that occurred during this period.

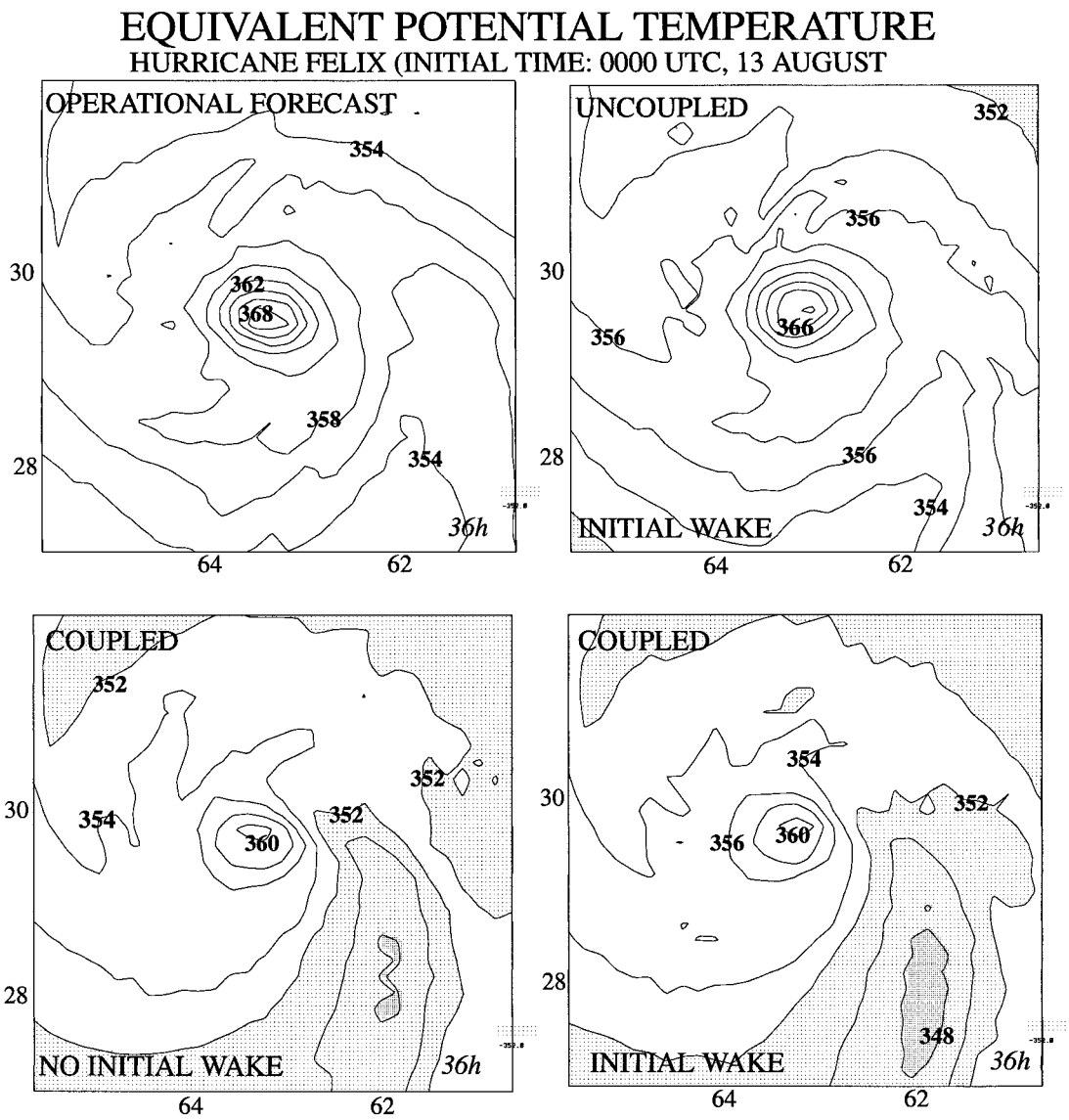

FIG. 16. The 36-h distribution of the equivalent potential temperature (K) at model level 18 ($\sigma = 0.995$, ~40 m height) for the operational forecast (uncoupled model without the initial cold wake; top, left) the uncoupled experiment with the initial wake (top, right), and the coupled experiments without (bottom, left) and with (bottom, right) the initial wake (0000 UTC 13 Aug initial time) for Hurricane Felix. The contour interval is 2 K with values less than 352 K and 348 K indicated by light and thick shading, respectively.

d. Hurricane Fran (1996)

The last series of forecasts involved two cases of Hurricane Fran starting at 0000 UTC 1 and 2 September 1996. During the 4-day period studied, Hurricane Fran moved in a west-northwest direction in the western Atlantic, north of the Caribbean. Four days prior to the start of the first integration (Fig. 17), Hurricane Edouard, which was an intense major hurricane, moved in nearly an identical path to Fran, producing a significant cold wake at the sea surface. During the first 2.5-day period of this study, Fran remained at nearly constant intensity with the minimum sea level pressure only varying between 976 and 981 hPa (Fig. 20). It is likely that the cold wake of Edouard was one of the primary reasons why Fran did not intensify during this period. However, the NCEP SST analysis, with its coarse resolution, did not show any sign of Edouard's wake and indicated SSTs of 28°–29°C in this region. The operational GFDL forecast without coupling incorrectly forecasted rapid intensification with the model storm deepening 40 hPa during the 2.5-day period.

To investigate the impact of Edouard's wake on the intensity of Hurricane Fran, two sets of coupled and noncoupled experiments were run for the forecast start-

TABLE 5. Difference in equivalent potential temperature and sea level pressure between the storm center and the storm periphery at 36 h; for all experiments in the Atlantic.

Hurricane	Expt	$\Delta\theta_e$ (K)	Δp_* (hPa)	$\frac{\Delta p_*}{\Delta\theta_e}$ (hPa K^{-1})
(0000 UTC 13 Aug 1995)				
Felix	Operational forecast	15.5	66	4.3
Felix	Not coupled, initial wake	14.7	66	4.5
Felix	Coupled, no initial wake	8.9	49	5.4
Felix	Coupled, initial wake	8.9	49	5.4
(0000 UTC 14 Aug 1995)				
Felix	Operational forecast	12.1	43	3.5
Felix	Not coupled, initial wake	12.0	39	3.3
Felix	Coupled, no initial wake	8.0	30	3.7
Felix	Coupled, initial wake	9.0	29	3.2
(0000 UTC 1 Sept 1996)				
Fran	Operational forecast	10.6	56	5.3
Fran	Not coupled, initial wake	9.0	44	4.9
Fran	Coupled, no initial wake	9.8	48	4.9
Fran	Coupled, initial wake	6.4	36	5.6
(0000 UTC 2 Sept 1996)				
Fran	Operational forecast	11.7	57	4.9
Fran	Coupled, initial wake	10.9	38	3.5
	Average ratio for Atlantic			4.5
	Ratio from Emanuel (1986)			3.3

ing at the 0000 UTC 1 September initial time. In the first set, Edouard's cold wake was generated during the ocean initialization by imposing the hurricane wind forcing from Edouard starting five days before the start of Fran's forecast. In the other set, the cold wake of Edouard was not imposed. (The uncoupled experiment without Edouard's cold wake was the operational forecast). The SST field at 72 h for both coupled runs is shown in Fig. 18, indicating the significant strong cooling produced by Hurricane Edouard in the ocean model. At the start of the forecast with Edouard's wake imposed, the SST near the storm center of Fran averaged about 2.5°C lower than the original NCEP analysis, with a maximum SST decrease of about 3°C in the region of the wake northwest of the storm. We were unable to verify the SST decrease in the vicinity of Fran's track. However, the model SST predictions were verified against AVHRR-derived SSTs observed to the north of the track of Fran (N. Nelson, Bermuda Biological Station for Research, 1997, personal communication). Figure 19 shows two cross sections of the SST distributions along 31° and 32°N comparing the ocean model simulations at the start of the coupled forecast (0000 UTC 1 September) and 3-day AVHRR composite images from 31 August through 2 September. In both cases a marked consistency is evident. The ocean model not only demonstrated high degree of skill in predicting the maximum SST decrease but, more importantly, the spatial extent of the cold wake was also simulated well. The model SST predictions were also consistent with measurements at the mooring located at 40.5°N, 70.5°W, which was about 110 km south of Cape Cod. The mooring was deployed during the Coastal Mixing and Optics project (T. Dickey 1997, personal communication). The eye of Hurricane Edouard passed within roughly 80 km of the mooring on 1 September 1996 when the storm was already weakening. The measurements indicate a temperature decrease from about 16°C to about 14°C at the depth of 10 m, which agreed well with the model SST prediction.

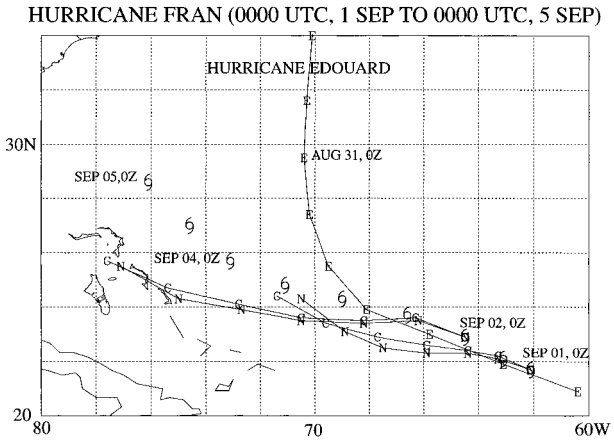

FIG. 17. The 72-h storm tracks (thin lines) for the two forecasts of Hurricane Fran made by the coupled model with Edouard's initial wake and the uncoupled operational forecast starting from 0000 UTC 1 and 2 Sep. The storm positions at 12-h intervals are indicated by the letters C (coupled) and N (uncoupled operational forecast). The observed positions of Fran at 12-h intervals are indicated by the storm symbols. The observed track of Hurricane Edouard is also indicated from the period 0000 UTC 28 Aug through 0000 UTC 1 Sep, with the storm position at 12-h intervals indicated by the letter E.

The forecasted time series of minimum sea level pres-

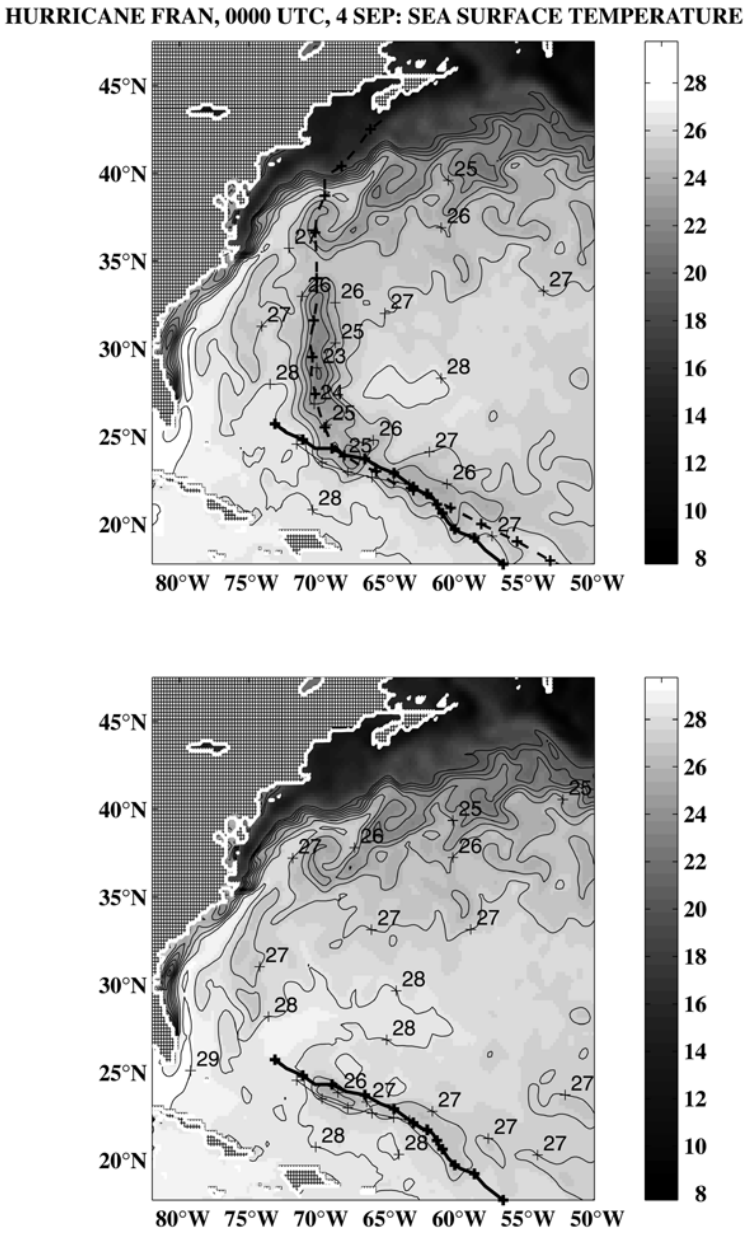

FIG. 18. The SST distribution (°C) at 72 h for the two coupled experiments for Hurricane Fran (0000 UTC 1 Sep initial time) run with (top) and without (bottom) Edouard's wake. The contour interval is 1°C with the lower SSTs indicated by the darker shading. The observed track starting from the 0000 UTC 28 Aug position and the 72-h forecasted track are shown by a thick and a thin solid line, respectively, with the observed and forecasted positions at 12-h intervals indicated by crosses. The observed track of Hurricane Edouard is also plotted with a thick dashed line, with Edouard's positions at 12-h intervals indicated by crosses.

sure for all sets of coupled and uncoupled experiments is shown in Fig. 20. In both experiments without inclusion of Edouard's wake, the storm began to intensify from the beginning, although at a reduced rate in the coupled forecast. By 36 h, the minimum sea level pressure had fallen to 953 and 960 hPa, respectively, compared to the observed value of 976 hPa. With inclusion of Edouard's wake, the intensity was considerably closer to the observed value, even without inclusion of the ocean coupling, with a minimum sea level pressure at 36 h of 967 and 973 hPa, respectively. This indicates that the effect of Edouard's cold wake on Fran's intensity was more important than the effect of the ocean coupling itself although inclusion of both effects was necessary

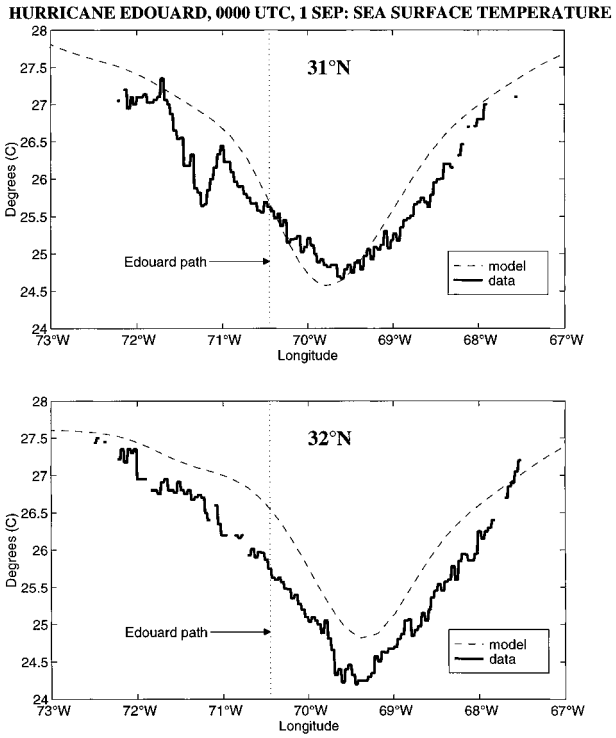

FIG. 19. Cross sections of SSTs (°C) along 31°N (top) and 32°N (bottom) from 3-day composite AVHRR satellite images, centered on 1 Sep (solid lines) and ocean model–predicted (dashed lines) SSTs at the beginning of the coupled model forecast. The location where the center of Edouard passed is indicated by the vertical lines.

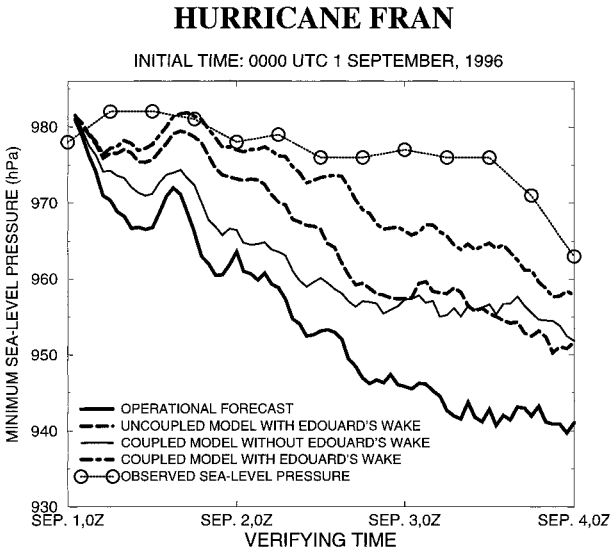

FIG. 20. Time series of minimum sea level pressure for the operational forecast (uncoupled model without Edouard's wake, thick solid line), the uncoupled experiment with Edouard's wake (dashed line), and the coupled experiments without (thin solid line) and with (dotted–dashed line) Edouard's wake (0000 UTC 1 Sep initial time), compared to observed values (dotted line, circles indicate values every 6 h).

to correctly forecast Fran's intensity. Beyond 36 h, the storm in the coupled forecast even with inclusion of Edouard's wake began to deepen. This was about one day before the actual intensification began as the forecasted track was well south of the actual track (Fig. 17), causing the model storm to move away too soon from Edouard's wake.

The accumulated evaporation for the four sets of experiments is presented next (Fig. 21) to evaluate the mechanisms leading to the intensity differences. The overall reduction of evaporation for each experiment was consistent with the decrease of intensity noted in Fig. 20. As expected, the decrease of evaporation was largest directly underneath the cold wake of Edouard, even in the experiment without the ocean coupling. Since the center of Fran moved just north of the track of Edouard and very near the center of its cold wake (Fig. 18), the accumulated evaporation north of the storm track was greatly reduced in these two experiments compared to the operational forecast. In both of the experiments with Edouard's wake, the evaporation just north of the 24-h storm center position was less than 1 cm compared to 2.5 cm (Fig. 21, top) for the operational model. With the effect of the ocean coupling also included (Fig. 21, bottom), further reduction of the SSTs reduced the evaporation south of the storm center to less than 0.75 cm near the 24-h position.

The effect of coupling on the boundary layer moist static energy is shown (Fig. 22) for these experiments at 36 h, when the center of Fran was located 100 km south of the center of Edouard's wake, with the hurricane moving away from the wake. Its effect in the storm's boundary layer (Fig. 22, right) is most evident northwest of the storm producing a 4–5 K lower equivalent potential temperature compared to the operational forecast. With the coupling included the equivalent potential temperature decreased to below 346 K over a fairly large area. The decrease of the equivalent potential temperature was much smaller south of the storm, providing the heat energy necessary to retain the storm intensity. Since the SST decrease at 36 h in the coupled experiment without Edouard's wake was less than 2°C (Fig. 18), the difference in the distribution of θ_e between the coupled and uncoupled experiments was much smaller (Fig. 22, left) than for Hurricane Felix (Fig. 16, left) as were the differences in $\Delta\theta_e$ and Δp_* (Table 5) between the coupled and uncoupled experiments, also computed at 36 h.

The values of $\Delta\theta_e$ again showed a good relationship with Δp_* in the Atlantic (Table 5), although on the average the ratio $\Delta p_*/\Delta\theta_e$ was larger (i.e., 4.5) than found for the experiments in the Gulf of Mexico (i.e., 3.6). This difference may be related to the difference in the environmental conditions in the two basins controlling the storm structure. For example, the equivalent potential temperature in the storm periphery was about

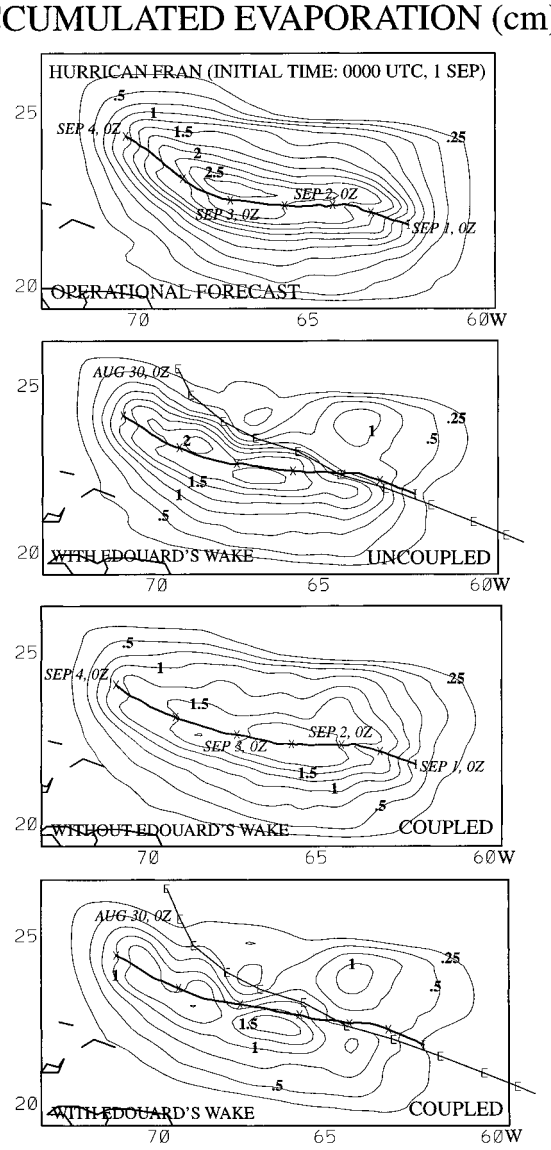

FIG. 21. Distribution of evaporation (cm) for the operational forecast (uncoupled model without Edouard's wake, top) the uncoupled experiment with Edouard's wake (upper middle), and the coupled experiment without (lower middle) and with (bottom) Edouard's wake, accumulated during passage of Hurricane Fran (0000 UTC 1 Sep initial time). The contour interval is 0.25 cm with the forecasted track indicated by the thick solid line. The observed track of Hurricane Edouard is also plotted from the period 1200 UTC 27 Aug through 0000 UTC 30 Aug, with the storm position at 6-h intervals indicated by the symbol E.

6 K greater in the Gulf of Mexico, the SSTs averaged 1°–1.5°C warmer, and the lower boundary layer mixing ratios were 2 gm kg^{-1} greater.

To evaluate the components contributing to the moist static energy for these experiments, the various terms of the moisture budget were evaluated next. This will clearly demonstrate the effect that the convergence of lower equivalent potential temperature air originating from the cold wake had on the storm intensity. The equation for the change of precipitiable water can be written

$$\overline{\frac{\partial}{\partial t}\int p_* r\,\frac{d\sigma}{g}} = -\overline{\int \nabla\cdot[(\mathbf{V}-\mathbf{C})p_* r]\,\frac{d\sigma}{g}} + \overline{\mathrm{EVAP}} - \overline{\mathrm{PREC}} + \overline{\mathrm{HDIF}}. \quad (3.2)$$

Here, the overbar denotes an area average, which was taken over a 300-km area surrounding the storm center. Since the results were not particularly sensitive to the domain size, this particular domain was chosen since it covered the latitudinal extent of most of the cold wake and was well beyond the eyewall region. The term r is the mixing ratio, $\mathbf{C}$ the mean storm movement vector, p_* the sea level pressure, $\mathbf{V}$ the vector wind, EVAP the evaporation rate, and PREC the precipitation rate. The term on the left-hand side denotes the change of total precipitable water, and the flux convergence of water vapor into the storm is represented by the first term on the right-hand side. The convergence of water vapor into the storm region through subgridscale horizontal diffusion (HDIF) was extremely small and was consequently ignored. The three terms remaining on the right side were computed at hour 6 of the forecast when the storms in the four experiments, located near the center of Edouard's wake, still had comparable intensity. The values (units of 10^{-6} cm s^{-1}) of the term for the flux convergence of moisture were 151, 135, 139, and 124 for the four experiments. The evaporation rate ranged from 15 for the operational forecast to 8, 11, and 6 for the three subsequent experiments, indicating a decrease of 60% between the first and fourth experiments. Although the actual magnitude of the decrease in the moisture supply due to the decreased evaporation is considerably smaller than the decrease from the advection term itself, weakening of the storm due to the decrease of the evaporation underneath the storm will decrease the radial inflow and directly impact the advection term, representing a positive feedback process between the two terms. It should be noted that the strength of the feedback depends on the SSTs below both the inner eyewall region and the outer regions of the storm near the storm periphery. To roughly balance the decreased moisture supply from the first two terms, the precipitation was significantly reduced with the average value in this region decreasing from 225 for the operational forecast to 187, 205, and 160 for the three experiments. This budget analysis indicates that the reduction of the supply of moist static energy into the eyewall region and, hence, reduction in storm intensity in the coupled experiments was caused by both the reduction in evaporation from underneath the storm as well as the reduction in the convergence of moist static energy.

Finally, with both Edouard's wake and the ocean coupling the intensity prediction was much improved start-

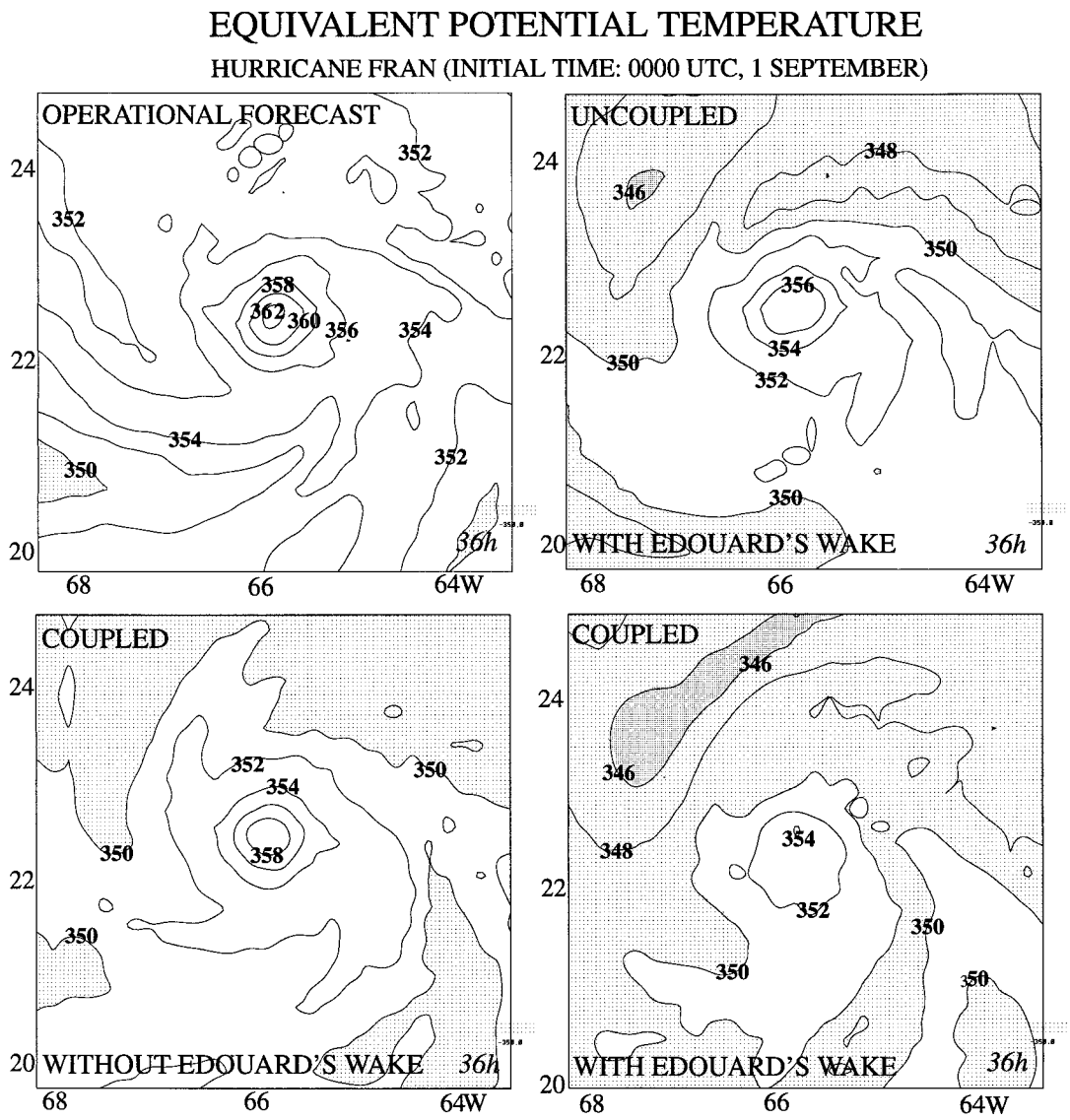

FIG. 22. The 36-h distribution of the equivalent potential temperature (K) at model level 18 ($\sigma = 0.995$, ~40 m height) for the operational forecast (uncoupled model without Edouard's wake; top, left), the uncoupled experiment with Edouard's wake (top, right), and the coupled experiments without (bottom, left) and with (bottom, right) Edouard's wake (0000 UTC 1 Sep initial time) for Hurricane Fran. The contour interval is 2 K with values less than 350 K and 346 K indicated by light and dark shading, respectively.

ing at both forecast periods (Fig. 23) compared to the operational forecasts. From the 0000 UTC 2 September initial time, the model also correctly predicted the rapid deepening that occurred on 3 September, as the storm began to move away from the cold wake of Edouard.

In summary, the wake of Hurricane Edouard greatly impacted the intensity of Fran during the period that the storm crossed or passed near to the wake. Since Fran's wake was completely absent from the global analysis, these results have demonstrated the need for an accurate and high-resolution SST analysis to improve intensity forecasts from a dynamical model.

e. Additional forecasts during the 1995–98 hurricane seasons

The effect of ocean coupling on hurricane intensity was recently investigated for more cases during the 1995–98 hurricane seasons. For these simulations the ocean computational domains in the Gulf of Mexico and western Atlantic described in section 2c were enlarged and a third domain was added in the central North Atlantic. At the beginning of each model run, an appropriate domain was automatically chosen depending on the initial and 72-h storm positions. Coupled and un-

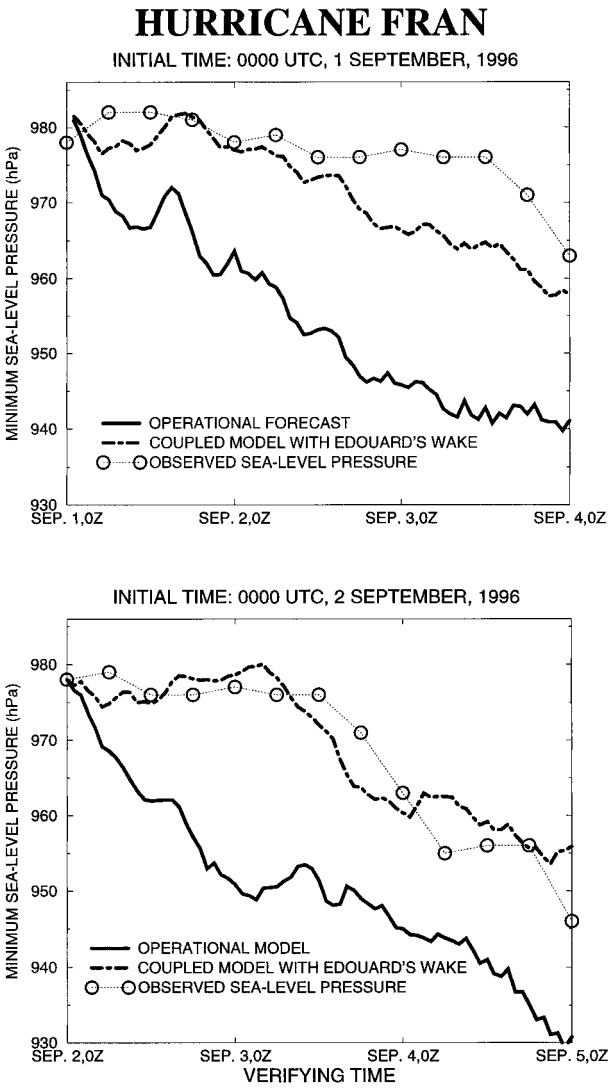

FIG. 23. Time series of minimum sea level pressure for the operational forecast (solid line) and coupled experiment with Edouard's wake (dotted–dashed line) compared to observed values (dotted line, circles indicate values every 6 h) for the two forecasts of Hurricane Fran.

coupled model simulations were first conducted for 28 forecasts made during the 1995–97 seasons. These cases were selected according to the following criteria: the track errors were less than 200 km at 36 h, and less than 250 km at 72 h, and the intensity errors were less than 6 hPa at the initial time. The selected storms were Hurricane Felix (three cases), Humberto (one), Iris (two), Luis (seven), Marilyn (two), in 1995; Hurricane Edouard (two), Fran (four), Isidore (three), Lili (one) in 1996; and Hurricane Erica (three) in 1997. In most of these cases (about 90%) the operational GFDL model overpredicted the intensity of the hurricanes measured by the minimum sea level pressure. The mean absolute error of the minimum sea level pressure was 16.4 hPa. In the coupled system, this error was reduced by about

TABLE 6. The GFDL operational and coupled hurricane–ocean model intensity forecast error based on 28 cases during the 1995–97 hurricane seasons and 135 cases during the 1998 season. Average absolute errors (hPa) are the difference between the forecast and observed values.

Verification		Average errors (hPa)		Improvement
Time	Cases	Operational	Coupled	(%)
1995–97 hurricane seasons				
12 h	28	8.71	9.01	−3.5
24 h	28	13.61	10.14	25.5
36 h	28	16.84	10.83	35.7
48 h	28	18.12	11.12	33.1
60 h	27	17.01	11.76	30.9
72 h	26	18.02	12.51	30.6
Avg improvement		15.39	11.06	25.4
1998 hurricane season				
12 h	135	12.86	10.98	14.6
24 h	131	16.81	13.11	22.1
36 h	124	18.96	13.86	26.9
48 h	120	21.94	15.03	31.5
60 h	112	25.10	17.42	30.6
72 h	105	27.60	19.10	30.8
Avg improvement		20.55	14.91	26.1

25%. More detailed error statistics at 12-h intervals are presented in Table 6 (top). Except at 12 h, reduction of the intensity forecast error, compared against the operational GFDL model, was found to be significant throughout the remaining 72-h period.

During the 1998 hurricane season the coupled hurricane–ocean system was run in near–real time mode when a direct data link with NCEP was established. Immediately after the integration of the operational GFDL model at NCEP all necessary data were transferred via the Internet from a Cray C-90 at NCEP to a Cray T-90 at the Naval Oceanographic Office Major Shared Resource Center where all numerical experiments were performed. The coupled model results were made available to the hurricane forecasters at the Tropical Prediction Center, via a dedicated Web site. In total, 135 forecasts were performed for Tropical Storm Alex (8 cases), Hurricane Bonnie (23), Hurricane Danielle (18), Hurricane Earl (6), Hurricane Georges (42), Hurricane Ivan (3), Hurricane Jeanne (10), and Hurricane Mitch (25). Error statistics every 12 h are provided in Table 6 (bottom). The mean absolute error for the forecasts of the minimum sea level pressure was reduced by about 26% compared to the operational GFDL model. Among a total of 727 forecast verification times, the operational GFDL model overpredicted the intensity (model storm was stronger than observed) in 536 cases (74%) an average of 22.4 hPa and underpredicted the intensity (model storm was weaker than observed) in 191 cases (26%) an average of 16.5 hPa. For those cases where the intensity was overpredicted, the average error was reduced by 8.5 hPa (38%) in the coupled model forecasts. For the cases where the intensity was underpredicted, inclusion of the ocean coupling lead to only

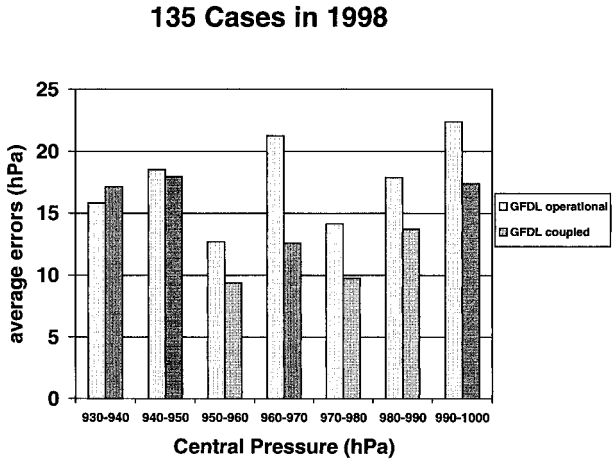

FIG. 24. Comparison between the operational and coupled GFDL model, for the average forecast error of minimum central pressure (hPa) at all forecast time periods, for 135 forecasts run during the 1998 Atlantic hurricane season. The comparison is made for seven categories of storm intensity.

a 2.5-hPa (14%) increase in the forecast error. This small increase in error was observed mainly for the strongest category of storm intensity in Fig. 24 (minimum sea level pressure less than 940 hPa) where the current $\frac{1}{6}^\circ$ horizontal resolution was not sufficient to resolve the extreme intensity. Since the ocean coupling always leads to weakening of the storm due to the negative feedback mechanism, this small degrading in the predicted storm intensity is expected for these cases. For example, in one forecast of Hurricane Mitch, which reached category 5 intensity over the Caribbean as it deepened to 906 hPa at 1800 UTC 26 October, the GFDL model predicted a minimum sea level pressure of 935 hPa while the hurricane in the coupled model deepened to 940 hPa. This resulted in a 16% increase in forecast error compared to the operational forecast. Since observations at the time indicated that the size of the hurricane eye was very small (~15 nm), the eye and eyewall structure clearly could not be resolved with the $\frac{1}{6}^\circ$ resolution. In this example, it is not surprising that despite Mitch's extreme intensity the ocean negative feedback remained relatively weak. This is due to a very small SST decrease (less then 0.3°C) underneath the storm associated with the deep ocean mixed layer in the Caribbean Sea.

Figure 24 shows a comparison between the operational and coupled GFDL model average errors in minimum sea level pressure for different storm intensities. On average, the coupled model improved the intensity forecasts for storms with a minimum sea level pressure greater than 940 hPa. The most significant improvements, about 60%, were achieved for the hurricanes with the intensity in a range of 960–970 hPa. For the weaker storms, with less turbulent mixing in the ocean, the SST decrease was usually smaller, and the effect on the storm intensity was reduced. More detailed analysis of these results is beyond the scope of this paper and will be the subject of future publications. Nevertheless, this much larger dataset confirms the conclusions from the case studies described above that have shown that the hurricane–ocean interaction is an important physical mechanism that effects the intensity of observed tropical cyclones.

4. Summary and conclusion

The effect of tropical cyclone–ocean interaction on the intensity of observed hurricanes was investigated by coupling the GFDL hurricane model with a high-resolution version of the Princeton Ocean Model. The experiments were run with and without inclusion of the coupling for two cases of Hurricane Opal (1995) and one case of Hurricane Gilbert (1988) in the Gulf of Mexico and two cases of Hurricanes Felix (1995) and Fran (1996) in the western Atlantic. The results confirmed the conclusions of earlier idealized studies regarding the impact of tropical cyclone–ocean interaction on hurricane intensity. In particular it was shown that the effect of the tropical cyclone–ocean interaction produced a significant cooling of the sea surface resulting in a substantial decrease in the evaporation and boundary layer moist static energy over the cold wake. This had a large effect on the storm intensity, particularly when the storms were moving slowly and the SST decrease was greater. In each of the seven forecasts made, inclusion of the ocean coupling generally lead to substantial improvements in the prediction of storm intensity measured by the storm's minimum sea level pressure. These results indicate that the effect of ocean coupling is one of the important mechanisms that govern the intensity of tropical cyclones. This strongly suggests that this effect needs to be included for reliable intensity predictions to be possible with the GFDL forecast system and probably dynamical models in general. This conclusion was verified with a much larger set of 163 forecasts made during the 1995–98 hurricane seasons.

After moving across the Yucatan Peninsula, Hurricane Gilbert deepened only 4 hPa during the 48-h period that it crossed the warm waters of the central Gulf of Mexico. Without the effect of the coupling, the operational GFDL model incorrectly forecasted continuous deepening of 25 hPa until the final landfall on the Mexican coast. With the coupling included the storm deepened only 10 hPa, which was much closer to the observed rate. This strongly suggests that the cooling of the SSTs was one of the primary factors that prevented Hurricane Gilbert from reintensifying as it moved across the very warm waters of the Gulf of Mexico under apparently favorable environmental conditions. Similarly, for Hurricane Opal, which moved very slowly during the period from 0000 UTC 2 October through 1200 UTC 3 October, both coupled model forecasts starting at 0000 UTC 1 and 2 October produced a large SST decrease just northwest of the Yucatan and only slow storm deep-

ening during this period, consistent with the observed deepening. In contrast, without the coupling, the operational model predicted rapid deepening (58 hPa from the 0000 UTC 2 October initial time). On 3 October, as Opal began to accelerate to the north, the hurricane rapidly began to strengthen. In the second forecast where the storm speed was well simulated, this trend was generally reproduced by the coupled model, although the rate of deepening was somewhat less than observed. In the first experiment in which the storm moved too quickly, the storm intensity was stronger than observed for the first 24 h of the forecast. This result was consistent with the previous idealized and observational studies, which showed that the storm translational speed was an important parameter affecting the amount of SST decrease caused by the moving hurricane. Nevertheless the importance of the effect of coupling on intensity predictions in the Gulf of Mexico was again demonstrated as the rapid intensification of Hurricane Opal, both model and observed, did not occur until the storm moved away from the waters with large SST decrease produced when the storm was slowly drifting in the southern Gulf of Mexico.

Improved intensity prediction was also achieved for Hurricane Felix in the Atlantic basin. The model resolution could not adequately reproduce the inner-core structure of Felix at its maximum intensity (i.e., 930 hPa), and the model's initial minimum sea level pressure was 17 hPa greater than observed. However, the storm in the operational model continually deepened during the next 24 h while the observed storm weakened over 30 hPa, partly affected by a large decrease in SSTs as the storm slowed its forward motion and curved north. In the coupled experiment, the model storm intensity was greatly impacted by the lower SSTs, and the storm quickly weakened to about 960 hPa and maintained a near-constant intensity for the remainder of the forecast. Although the rate of weakening was much too rapid during the first 12 h, the agreement with the observed storm intensity was excellent during the last half of the forecast.

In the final series of experiments involving Hurricane Fran, two forecasts were made starting at 0000 UTC 1 and 2 September during which time Fran's intensity was influenced by the cold wake of Hurricane Edouard, which moved in nearly an identical path four days earlier. Since the wake of Hurricane Edouard was not resolved by the coarse resolution of the NCEP SST analysis, the operational GFDL model incorrectly forecasted 40-hPa deepening while Fran remained at nearly constant intensity. To investigate the impact of Edouard's wake two sets of coupled and noncoupled experiments were run from the first forecast time. In the first set, Edouard's cold wake was generated before the start of the forecast. In the second set of experiments Edouard's wake was not included. The wake significantly impacted the intensity of Fran during the period that it crossed the wake and the model storm intensity was considerably closer to the observed value, even without the ocean coupling. This demonstrates the importance of the effect of Edouard's cold wake on the intensity of Fran. With inclusion of both the wake and the ocean coupling the intensity prediction was much improved starting at both forecast periods. In the coupled experiment starting from the 0000 UTC 2 September initial time, the model also predicted the rapid deepening that occurred once Fran began to move away from the cold wake of Edouard. On the previous day the storm began to deepen one day too soon since the forecasted track was south of the actual track and the model storm moved away from the wake too soon. Therefore, for this storm both an accurate initial SST analysis as well as the inclusion of the ocean coupling proved essential for accurate hurricane intensity prediction using a dynamical model.

Since the decrease in the SST was the primary mechanism affecting the storm intensity caused by the ocean interaction, the sensitivity of the GFDL model to SSTs should be carefully evaluated. In modeling studies of tropical storm genesis (Tuleya and Kurihara 1982) threshold values of 26°–27°C in the SST were necessary in the GFDL model for development of a tropical storm from an easterly wave. This agreed well with the threshold values observed from climatology (Wendland 1977). In recent studies of Knutson et al. (1998) and Shen et al. (2000), a series of sensitivity tests have been conducted with the GFDL model to assess the effect of SST increase associated with global warming on hurricane intensity. For an SST increase of 2°C, the simulations indicate an intensification of 7–20 mb for central pressure. The latter is comparable with theoretical estimates of the maximum potential intensity by Emanuel (1988) and Holland (1997). Emanuel's method gives an increase in intensity of 23 and 10 hPa, respectively, assuming either thermodynamically reversible or pseudoadiabatic ascent of air parcels. Holland's method gives an increase of 18 hPa using the same thermodynamic profiles.

The effect of local SST cooling on hurricane intensity in the current study was actually somewhat less than that from theoretical estimates based on Emanuel (1988) and Holland (1997), which both give about a 30-hPa rise in central pressure for a 1°C SST decrease near the eyewall. In the simulations presented in this study, the most dramatic effect of ocean coupling was a 40-hPa increase in central pressure that occurred for Hurricane Opal on 0000 UTC 3 October, which had about a 3°C SST decrease, averaged over a 100-km-radius circle under the storm. Nevertheless, based on these comparisons we can conclude that the impact on the hurricane intensity caused by the SST decrease produced by the GFDL model was reasonable, at least within the bounds of these theoretical results and idealized experiments.

The mechanisms contributing to the differences in storm intensity due to the ocean coupling were examined for the various storms presented in this study by

also analyzing the changes in the moist static energy. Although the area of maximum SST decrease was found to occur over a relatively small area behind the storm center, it was shown that it led to a significant decrease in equivalent potential temperature. Analysis of the moisture budget for Hurricane Fran demonstrated that the reduction of the supply of moist static energy into the eyewall was caused by both the reduction in evaporation from underneath the storm and the reduction in the convergence of moist static energy into the storm region from the outer storm periphery. A good correlation was found between the changes in the equivalent potential temperature and the sea level pressure measured between the storm center and the outer periphery. Nevertheless, although the supply of moist energy is crucial in the maintenance of the storm intensity, other factors (e.g., static stability, the upper-level flow field, etc.) are also important suggested by the variation in the ratio of these two terms between individual experiments.

Changes in the storm track by the ocean coupling were not the topic of the present study. However, it should be pointed out that the differences in the storm track were small between forecasts run with and without ocean coupling for Hurricanes Gilbert, Opal, and Felix, despite the large intensity differences. Analysis of the storm's circular averaged tangential flow (figures not shown) indicated little differences in the winds in the outer storm radii (300–700 km) between the storms in the coupled and uncoupled experiments. Using a nondivergent, barotropic numerical model, Fiorino and Elsberry (1989) found largest changes in the storm track related to differences in the tangential wind profiles at these storm radii, with little sensitivity to storm track due to changes in the wind profile at the inner storm radii. Significant difference in storm track for Fran only occurred between the coupled experiment with Edouard's wake and the operational forecast. For the two experiments of Fran, this lead to a reduction in track error of about 12% at the 24-, 48-, and 72-h time periods when the coupling and the initial wake of Edouard was added. A more thorough investigation on the mechanisms contributing to changes in the track between the coupled and uncoupled models will be reserved for future studies.

During the 1998 hurricane season, the new GFDL hurricane–ocean coupled model described in this paper was run in near–real time for 135 cases in the Atlantic and Gulf of Mexico. Improved intensity forecasts were again achieved with the mean absolute error in the forecast of minimum sea level pressure reduced by about 26% compared to the operational GFDL model. The coupled model improved the intensity forecasts for all storms with minimum sea level pressure higher than 940 hPa with the most significant improvement (~60%) in the intensity range of 960–970 hPa. Similar improvements were obtained for a 28-case sample size during the 1995–97 seasons. Both of these much larger sample sets confirmed the conclusion based on the case studies presented here that the hurricane–ocean interaction is an important physical mechanism that can significantly effect the intensity of observed tropical cyclones. These results also suggest that inclusion of hurricane–ocean coupling is necessary for accurate tropical cyclone intensity prediction using the GFDL hurricane model as well as dynamical models in general.

This study has revealed other areas of model improvement that will likely need to be addressed before the GFDL hurricane prediction system can become a skillful predictor of hurricane intensity. First, since the current $\frac{1}{6}^{\circ}$ resolution was unable to adequately resolve the interior of intense storms such as Hurricane Felix and Opal in 1995, the need to increase the finest resolution of the innermost grid was identified. As a result, during the 1998 hurricane season, the intensity of storms below 940 hPa usually were underestimated, resulting in a small degradation in the intensity forecast by the coupled model compared to the operational version. Another future area for model improvement is to increase the model's vertical resolution. Tests with a new version of the model with greater vertical resolution have recently begun at GFDL. In one experiment for Hurricane Opal, in which the vertical resolution was increased from 18 to 42 levels, the hurricane response to the ocean coupling was practically unaffected, although the storm became slightly more intense. Changes in the model physics for both the atmosphere and oceans are also being evaluated. When the model's convective parameterization scheme was replaced by a scheme developed by Emanuel and Živković-Rothman (1999), in the same forecast for Hurricane Opal, the storm became less intense although the ocean coupling still greatly reduced the model's positive intensity bias. Finally, refinements to the structure of the vortex generated in the current GFDL initialization scheme are being formulated. To address this last issue, a new scheme for vortex generation has been developed and is also currently being tested at GFDL, yielding positive results. A simplified version of this scheme was made operational in the 1998 season and likely contributed to a reduction in intensity error especially during the first day of the forecast.

Acknowledgments. The authors would like to thank J. Mahlman for his continuous support of the Hurricane Dynamics Project at GFDL. They would also like to express their appreciation to Yoshio Kurihara, Robert E. Tuleya, and Tal Ezer for their comments and criticisms of an earlier version of this manuscript. The authors are grateful to N. Nelson, L. Shay, and T. Dickey for providing the ocean observational data. Programming assistance from S. Frolov is also gratefully acknowledged. Isaac Ginis was supported by the National Science Foundation through Grant ATM 9714412 and the U.S. Office of Naval Research through Grant N000149610758. Partial support for this work was also provided by the Risk Prediction Initiative at the Ber-

muda Biological Station for Research, Inc. Finally, additional computational support has been provided by the Department of Defense High Performance Computing Modernization Program at the Naval Oceanographic Office (NAVOCEANO) Major Shared Resource Center.

REFERENCES

Bender, M. A., I. Ginis, and Y. Kurihara, 1993a: Numerical simulations of tropical cylone–ocean interaction with a high-resolution coupled model. *J. Geophys. Res.,* **98,** 23 245–23 263.

——, R. J. Ross, R. E. Tuleya, and Y. Kurihara, 1993b: Improvements in tropical cyclone track and intensity forecasts using the GFDL initialization system. *Mon. Wea. Rev.,* **121,** 2046–2061.

Black, P. G., 1983: Ocean temperature changes induced by tropical cyclones. Ph.D. dissertation, The Pennsylvania State University, 278 pp.

Blumberg, A. F., and G. L. Mellor, 1987: A description of a three-dimensional coastal ocean circulation model. *Three-dimensional Coastal Ocean Models,* N. Heaps, Ed., Vol. 4, Amer. Geophys. Union, 1–16.

Chang, S. W., and R. A. Anthes, 1978: Numerical simulations of the ocean's nonlinear baroclinic response to translating hurricanes. *J. Phys. Oceanogr.,* **8,** 468–480.

——, and ——, 1979: The mutual response of the tropical cyclone and the ocean. *J. Phys. Oceanogr.,* **9,** 128–135.

Dickey, T. D., and Coauthors, 1998: Upper ocean temperature response to Hurricane Felix as measured by the Bermuda Tested Mooring. *Mon. Wea. Rev.,* **126,** 1195–1201.

Derber, J., H. Pan, J. Alpert, P. Caplan, G. White, M. Iredell, Y. Hou, K. Campana, and S. Moorthi, 1998: Changes to the 1998 NCEP operational MRF model analysis/forecast system. Tech. Procedures Bull. 449. [Available from National Centers for Environmental Prediction, W/NP23, World Weather Building, Washington, DC 20233; or online at http://www.nws.noaa.gov/om/tpb/indexb.htm.]

Emanuel, K. A., 1986: An air–sea interaction theory for tropical cyclones. Part I: Steady-state maintenance. *J. Atmos. Sci.,* **43,** 585–604.

——, 1988: Toward a general theory of hurricanes. *Amer. Sci.,* **76,** 371–379.

——, and M. Živković-Rothman, 1999: Development and evaluation of a convection scheme for use in climate models. *J. Atmos. Sci.,* **56,** 1766–1782.

Falkovich, A. I., A. P. Kain, and I. Ginis, 1995: The influence of air–sea interaction on the development and motion of a tropical cyclone: numerical experiments with a triply nested model. *Meteor. Atmos. Phys.,* **55,** 167–184.

Fiorino, M., and R. L. Elsberry, 1989: Some aspects of vortex structure related to tropical cyclone motion. *J. Atmos. Sci.,* **46,** 975–990.

Ginis, I., and Kh. Zh. Dikinov, 1989: Modelling of the Typhoon Virginia (1978) forcing on the ocean. *Meteor. Hydrol.,* **7,** 53–60.

——, ——, and A. P. Khain, 1989: A three dimensional model of the atmosphere and the ocean in the zone of a typhoon. *Dokl. Akad. Sci. USSR,* **307,** 333–337.

——, L. K. Shay, L. M. Rothstein, and S. A. Frolov, 1996: Numerical simulations of the ocean response to Hurricane Gilbert using airborne field observations. Preprints, *Eighth Conf. on Air–Sea Interaction,* Atlanta, GA, Amer. Meteor. Soc., 33–37.

Hodur, R. M., 1997: The Naval Research Laboratory's Coupled Ocean/Atmosphere Mesoscale Prediction System (COAMPS). *Mon. Wea. Rev.,* **125,** 1414–1430.

Hogg, N. G., R. S. Pickart, R. M. Hendry, and W. J. Smethie, 1986: The northern recirculation gyre of the Gulf Stream. *Deep-Sea Res.,* **33,** 1139–1165.

Holland, G. J., 1997: The maximum potential intensity of tropical cyclones. *J. Atmos. Sci.,* **54,** 2519–2541.

Khain, A. P., and I. Ginis, 1991: The mutual response of a moving tropical cyclone and the ocean. *Beitr. Phys. Atmos.,* **64,** 125–141.

Knutson, T. R., R. E. Tulyea, and Y. Kurihara, 1998: Simulated increase of hurricane intensities in CO_2-warmed climate. *Science,* **279,** 1018–1020.

Kurihara, Y., 1973: A scheme of moist convective adjustment. *Mon. Wea. Rev.,* **101,** 547–553.

——, and M. A. Bender, 1980: Use of a movable nested mesh model for tracking a small vortex. *Mon. Wea. Rev.,* **108,** 1792–1809.

——, ——, R. E. Tuleya, and R. J. Ross, 1995: Improvements in the GFDL hurricane prediction system. *Mon. Wea. Rev.,* **123,** 2791–2801.

——, R. E. Tuleya, and M. A. Bender, 1998: The GFDL hurricane prediction system and its performance in the 1995 hurricane season. *Mon. Wea. Rev.,* **126,** 1306–1322.

Lacis, A. A., and J. E. Hansen, 1974: A parameterization for the absorption of solar radiation in the earth's atmosphere. *J. Atmos. Sci.,* **31,** 118–133.

Large, W. G., and S. Pond, 1981: Open ocean momentum flux measurements in moderate to strong wind. *J. Phys. Oceanogr.,* **11,** 324–336.

Lawrence, M. B., C. J. McAdie, and J. M. Gross, 1997: Operational tropical cyclone track forecast verification at the National Hurricane Center. Preprints. *22d Conf. on Hurricanes and Tropical Meteorology,* Fort Collins, CO, Amer. Meteor. Soc., 475.

Leaman, K. D, R. L. Molinari, and P. S. Vertes, 1987: Structure and variability of the Florida Current at 27°N: April 1982–July 1984. *J. Phys. Oceanogr.,* **17,** 565–583.

Mellor, G. L., 1991: An equation of state for numerical models of oceans and estuaries. *J. Atmos. Oceanic Technol.,* **8,** 609–611.

——, 1998: User's guide for a three-dimensional, primitive equation, numerical ocean model. Program in Atmospheric and Oceanic Sciences, Princeton University, 35 pp. [Available online at http://www.aos.princeton.edu/WWWPUBLIC/htdocs.pom/.]

——, and T. Yamada, 1974: A hierarchy of turbulence closure models for planetary boundary layers. *J. Atmos. Sci.,* **31,** 1791–1806.

——, and ——, 1982. Development of a turbulence closure model for geophysical fluid problems. *Rev. Geophys. Space Phys.,* **20,** 851–875.

——, C. Mechoso, and E. Keto, 1982: A diagnostic calculation of the general circulation of the Atlantic Ocean. *Deep-Sea Res.,* **29,** 1171–1192.

——, T. Ezer, and L.-Y. Oey, 1994: The pressure gradient conundrum of sigma coordinate ocean models. *J. Atmos. Oceanic Technol.,* **11,** 1126–1134.

Nelson, N. B., 1998: Spatial and temporal extent of sea surface temperature modifications by hurricanes in the Sargasso Sea during the 1995 season. *Mon. Wea. Rev.,* **126,** 1364–1368.

NOAA, 1979: Meteorlolgical criteria for standard project hurricane and probable maximum hurricane wind fields, Gulf of Mexico and east coast of the United States. NOAA Tech. Rep. NWS 23, Washington DC, 320 pp.

Price, J. F., 1981: Upper ocean response to a hurricane. *J. Phys. Oceanogr.,* **11,** 153–175.

Reynolds, R. W., and T. M. Smith, 1994: Improved global sea surface temperature analyses using optimum interpolation. *J. Climate,* **7,** 929–948.

Richardson, P. L., 1985: Average velocity and transport of the Gulf Stream near 55 W. *J. Mar. Res.,* **43,** 83–111.

Schwarzkopf, M. D., and S. B. Fels, 1991: The simplified exchange method revistied: An accuarate, rapid method for computation of infrared cooling rates and fluxes. *J. Geophy. Res.,* **96,** 9075–9096.

Shay, L. K., P. G. Black, A. J. Mariano, J. D. Hawkins, and R. L. Elsberry, 1992: Upper ocean response to Hurricane Gilbert. *J. Geophys. Res.,* **97,** 20 227–20 248.

——, A. J. Mariano, S. D. Jacob, and E. H. Ryan, 1998a: Mean and near-inertial ocean current response to Hurricane Gilbert. *J. Phys. Oceanogr.,* **28,** 858–889.

——, G. J. Goni, F. Marks, J. J. Cione, and P. G. Black, 1998b: Role of warm ocean features on intensity change of Hurricane Opal. Preprints, *Symp. on Tropical Cyclone Intensity Change*, Phoenix, AZ, Amer. Meteor. Soc., 131–138.

Shen, W., R. E. Tuleya, and I. Ginis, 2000: A sensitivity study of atmospheric static stability on GFDL model hurricane intensity: Implications for global warming. *J. Climate,* **13,** 109–121.

Smagorinsky, J., 1963: General circulation experiments with primitive equations. I. The basic experiments. *Mon. Wea. Rev.,* **91,** 99–164.

Sutyrin, G. G., and A. P. Khain, 1979: Interaction of the ocean and the atmosphere in the area of moving tropical cyclone. *Dokl. Akad. Nauk SSSR,* **249,** 467–470.

——, and ——, 1984: On the effect of air-ocean interaction on intensity of moving tropical cyclone. *Atmos. Oceanic Phys.,* **20,** 697–703.

Tuleya, R. E., 1994: Tropical storm development and decay: sensitivity to surface boundary conditions. *Mon. Wea. Rev.,* **122,** 291–304.

——, and Y. Kurihara, 1982: A note on the sea surface temperature sensitivity of a numerical model of tropical storm genesis. *Mon. Wea. Rev.,* **110,** 2063–2069.

Wendland, W. M., 1977: Tropical storm frequencies related to sea surface temperature. *J. Appl. Meteor.,* **16,** 477–481.

Xu, J., and W. M. Gray, 1982: Environmental circulations associated with tropical cyclones experiencing fast, slow and looping motion. Colorado State University Atmos. Sci. Paper 346, 273 pp. [Available from Colorado State University, Fort Collins, CO 80523.]